NASA CR-165,605

NASA Contractor Report 165605

NASA-CR-165605
19820020533

EFFECTS OF COBALT ON THE MICROSTRUCTURE OF UDIMET 700

Mayer Abraham Engel

Purdue University
West Lafayette, Indiana

LIBRARY COPY

JUL 30 1982

LANGLEY RESEARCH CENTER
LIBRARY, NASA
HAMPTON, VIRGINIA

June 1982

Prepared for

NATIONAL AERONAUTICS AND SPACE ADMINISTRATION

Lewis Research Center
Under Grant NAG3-57

TABLE OF CONTENTS

N82-28409 #

I. INTRODUCTION

Nickel-base superalloys are used extensively in many high temperature applications including aircraft, marine, and industrial gas turbines as well as other energy producing devices. They are noted for their outstanding strength and ability to maintain adequate ductility at elevated temperatures. Furthermore, these alloys are resistant to high temperature creep, impact, mechanical, and thermal fatigue, oxidation and corrosion.[1]

In order to achieve the desired high temperature properties, nickel-base superalloys are usually quite complex in microstructure and composition. Aside from nickel, these alloys may contain considerable amounts of the following elements:

chromium (Cr)	molybdenum (Mo)
cobalt (Co)	tungsten (W)
aluminum (Al)	tantalum (Ta)
titanium (Ti)	niobium (Nb)
vanadium (V).	

Minor alloying elements may include:

carbon (C)	boron (B)
zirconium (Zr)	hafnium (Hf)[1,2]

At current rates of consumption, many of the known sources of the major alloying elements will be depleted within fifty years.[2-4] Recently, cobalt, chromium, molybdenum, and tantalum have been

classified as "strategic materials" due to inherent uncertainties in their supply and availability.[5-7] This situation has intensified research activities in the development of superalloys with comparable high temperature properties, but with lesser amounts of these strategic elements.[7]

In particular, the role of cobalt is of great importance because of its wide use in nickel-base superalloys and because of the uncertainties of its availability and high cost.[8-13] Consequently, it is of specific interest to reduce the amount of cobalt in these superalloys without degrading their essential high temperature properties. Initially, this will require a fundamental understanding of the effect of cobalt in these alloy systems.

This study deals specifically with cobalt and its effect upon the microstructure of Udimet 700, a very versatile nickel-base superalloy used for both gas turbine blade and disk applications. Of specific interest are the effects of cobalt content upon the lattice parameters of the gamma (γ) matrix, primary and secondary gamma prime (γ'), and the γ/γ' lattice mismatch. In addition to the aforementioned interests, the distribution, composition, and relative quantities of the resultant phases are also investigated.

II. LITERATURE REVIEW

2.1. Strengthening Mechanisms in Superalloys

Many of the current nickel-base superalloys are capable of withstanding operating temperatures up to eighty percent of their absolute melting temperatures (Tm). This excellent high temperature capability is due to the precipitation and solid solution strengthening mechanisms imparted by judicious additions of various alloying elements.[14]

Nickel-base superalloys are primarily strengthened by the precipitation of γ', an fcc A_3B type intermetallic phase written as Ni_3Al. γ' coherently precipitates in the fcc γ matrix, resulting in a γ/γ' lattice mismatch which is usually less than one percent. This allows for homogeneous nucleation of a γ' precipitate with low surface energy and excellent long-time stability.[1]

The γ' phase, Ni_3Al, is very unusual in that it retains its strength with increasing temperature, thereby enhancing the mechanical properties of the alloy at elevated temperatures. Titanium and niobium can commonly substitute for aluminum in the γ' crystal structure, whereas cobalt replaces only nickel. Other elements found in the γ' include tantalum, tungsten, chromium and hafnium.[1]

The nickel-base fcc γ matrix is solid-solution strengthened mainly by additions of chromium, tungsten, and molybdenum. Other solid-solution elements found in the γ include cobalt, iron, vanadium, aluminum, and titanium.[15-17] Excessive amounts of elements such as

chromium, tungsten, molybdenum, and/or iron can form detrimental phases; therefore, the content of these elements must be carefully controlled.[1]

Solid-solution strengthening of the nickel-base austenitic γ matrix is directly related to the lattice expansion created by atomic diameter oversize.[18,19] The atomic diameters of the solid-solution elements mentioned above, differ from that of nickel by 1 to 13 percent. These elements have also been shown to lower the stacking fault energy, making cross-slip more difficult in the γ, and thereby strengthening the γ matrix.[20]

2.2. Phases Found in Superalloys

The majority of nickel-base superalloys in use today are variations of the basic nickel-chromium solid-solution γ matrix. Because of the large quantity of alloying elements present in superalloys, these alloys may form a number of phases aside from γ and γ', including MC, $M_{23}C_6$, M_6C, M_7C_3, M_3B_2, sigma, mu, or Laves.[1]

Dependent upon the aluminum and titanium content, nickel-base superalloys may contain from 15 to 60 volume percent of the fcc γ' phase. Coarse (primary) γ' forms at the onset of solidification in a high temperature range, while the fine-strengthening (secondary) γ' forms upon cooling and during low temperature heat treatments. Hence, the size and volume fraction of γ' can be controlled by heat treatments designed to enhance mechanical properties.[1]

Many classes of carbides are found in superalloys. The distribution and morphology of these hard and brittle phases have a direct effect upon the mechanical properties of the material. Carbides have been shown to have a significant and beneficial effect upon rupture strength

at high temperatures. However, undesirable morphologies such as continuous grain boundary films, needles, and plates tend to reduce ductility and rupture life.[1]

The primary MC carbide is a fcc phase which forms during the initial stages of solidification in superalloys.[1,21] These primary carbides contain titanium, tantalum, niobium, hafnium, or tungsten, and are found in both intergranular and transgranular locations. Upon heat treatment or in service operation at elevated temperatures, the MC can decompose releasing carbon and thereby triggering a number of important secondary carbide reactions. The dominant secondary carbide reaction involves the formation of the chrome rich $M_{23}C_6$ carbide, which preferentially precipitates in the grain boundaries, in the temperature range of 760-1010°C (1400-1850°F). However, in some instances $M_{23}C_6$ carbides have been observed in transgranular locations.

In alloys without molybdenum, the Cr_7C_3 secondary carbide forms. Alloys containing a sum of the molybdenum and tungsten contents greater than 6 weight percent can form the secondary carbide, M_6C, in a temperature range of 870-1180°C (1600-2150°F).[1]

The M_3B_2 boride is a primary phase rich in chromium, molybdenum, and tungsten, with lesser amounts of nickel, titanium, and cobalt. It forms during solidification when the boron level is 120 ppm or higher. The M_3B_2 borides may occur in either transgranular or intergranular positions. When located in the grain boundaries, these borides tend to reduce grain boundary tearing when the material is subjected to stress.[1]

Plate-like phases such as sigma, mu, and Laves are also found in superalloys. These phases are referred to as Topologically Close

Packed (TCP) phases, consisting of close-packed layers of atoms found only in certain crystallographic planes. These hard undesirable phases, containing chromium, molybdenum or cobalt, may nucleate in the vicinity of grain boundaries or in transgranular locations during heat treatment and service. Because of their brittle nature and plate-like morphology, TCP phases readily propagate cracks and are therefore detrimental to the mechanical properties of the alloy.[1]

2.3. Effect of Cobalt in Nickel-Base Superalloys

Only a few studies have investigated the specific effects of cobalt in superalloys.[22-28] Because cobalt can participate in so many of the microstructural reactions found in superalloys, the role of cobalt may vary from alloy to alloy. Furthermore, comparison of results from previous studies can be complicated because of varying alloy compositions, solidification conditions, and different thermal-mechanical processing.

In 1964, Heslop made a comparative study of Niminoc Alloy 80A, a Ni-Cr cobalt-free system and Nimonic Alloy 90, a Ni-Cr-Co system containing 17 weight percent cobalt.[22] Heslop concluded that cobalt additions increased the high temperature strength of the alloying systems considered by decreasing the solubility of the aluminum and titanium in the matrix which increased the amount of γ' precipitated.[22,23] Furthermore, the presence of cobalt decreased the amount of grain boundary precipitation of the $M_{23}C_6$ carbides by increasing the solubility of carbon in the matrix. This is significant as the form, morphology, and distribution of carbide precipitates in superalloy grain boundaries

are known to affect creep and stress rupture as well as fatigue crack initiation and propagation properties.[1] The precipitation of carbides in the grain boundaries has been shown to increase the strength of superalloys as long as the carbides remain discrete. Excessive precipitation of grain boundary carbides is deleterious to the mechanical properties of superalloys as continuous hard phases are highly prone to cracking which leads to brittle failure. Heslop also indicated that cobalt additions in the Ni-Cr-Co system decrease the stacking fault energy of the γ matrix which in turn exerts a solid-solution strengthening effect and thereby suppresses cross-slip which promotes strengthening.[22,23]

A study by Mauer, et al., on the effects of systematic substitution of nickel for cobalt in Waspaloy showed that the precipitation of grain boundary $M_{23}C_6$ carbides at 843°C (1550°F) increased as cobalt was reduced, very similar to Heslop's observations.[22,24] However, in the as-rolled condition prior to heat treatment the amount of MC carbides increased with decreasing cobalt content.

Maurer, et al.,[24] also noted that the volume fraction of γ' in Waspaloy decreased slightly with decreasing cobalt content similar to Heslop.[22] However, the γ' solvus temperatures remained unchanged. Other observed effects of decreasing cobalt content included a slight decrease in yield and tensile strengths, increased creep rate, and a shorter rupture life. These effects were thought to result from a combination of a smaller volume fraction of γ', changes in carbide precipitation,and higher stacking fault energies.[1,22,24]

Nathal and Maier recently concluded,as part of a NASA program, a study on the effect of decreased cobalt in Mar M-247, a nickel-base superalloy nominally containing 10.0 wt.% cobalt.[25] As cobalt was

removed from the alloy, the carbide precipitation increased and a grain boundary carbide film was formed. Other consequences of reduced cobalt content included a decrease in the volume fraction of γ' (similar to Heslop and Mauer), an increase in γ' solvus temperature, and a coarsening of the γ' precipitates. Also noted were changes in the elemental partitioning between the γ' and γ. As cobalt was reduced, an increase of titanium and tungsten was observed in the γ', while the chromium and aluminum contents of the γ matrix decreased.

The mechanical properties of the low cobalt Mar M-247 were also investigated by Nathal and Maier.[25] Slight increases in the yield and tensile strengths were noted in the 5.0 wt.% cobalt alloy. As the cobalt content was reduced from the nominal 10.0 wt.% level, the creep rate increased and the stress rupture life was shortened. However, these mechanical properties may not actually be a direct consequence of cobalt content as porosity was observed in all of the castings. Previous studies have indicated that porosity increases creep rate and causes degradation of the mechanical properties in superalloys.[29]

Whelan found that the addition of cobalt in Inconel 617, a nickel-base superalloy, is not essential to achieve acceptable high temperature rupture life.[26]

Lund, et al., investigated the effect of cobalt upon sigma formation in Mar M421 and found that when cobalt is present below 5 wt.%, the precipitation of sigma phase, and epsilon α Cr or "J" phase is inhibited.[28] When the cobalt enters the γ matrix and γ', chromium is displaced from the γ' to the γ, while nickel, titanium and aluminum are displaced from the γ to the γ'. This presumably stabilizes the fcc structure of the γ' and decreases the formation of sigma. However,

in amounts above 5 wt.%, cobalt was observed to actively participate in sigma formation at the expense of chromium. Increasing cobalt content promoted sigma formation, reduced the sigma lattice parameter and decreased the coarsening kinetics of the γ'.

III. EXPERIMENTAL PROCEDURE

3.1. Materials

Five experimental heats of Udimet 700 containing 0.1, 4.3, 8.6, 12.8, and 17.0 wt.% cobalt were prepared by the Special Metals Corporation (SMC), a division of Allegheny Ludlum Industries located in New Hartford, New York. Each of the 70 kg heats were vacuum induction melted (VIM) and cast into 10.2 cm round ingots. These ingots were subsequently used as consumable electrodes in the vacuum arc remelt (VAR) furnace. The resultant VAR ingots measuring 15.3 cm in diameter were then cogged into 6.3 cm round cornered square bars and hot rolled down to a 6.3 cm wide by 1.8 cm flat plate. Specimen blanks were then cut from the plates and heat treated for mechanical property testing and phase analysis. The compositions of the experimental alloys shown in Table I were determined by quantitative wet chemistry, atomic adsorption, mass spectroscopy and interstitial analysis techniques. The alloy compositions vary only in the amount of cobalt which was substituted for by nickel.

3.2. Heat Treatment

When Wrought Udimet 700 is used for turbine disk applications a fine-grained microstructure is essential. This is accomplished by initially heat treating the material just below the γ' solvus temperature resulting in a partial solutioning of the γ'. The remaining

TABLE I. Experimental Alloy Compositions (wt.%)

Heat No.	Ni	Co	Cr	Mo	Ti	Al	C	B	Fe
D5-1884	72.1	< 0.1	15.1	5.0	3.5	4.12	0.06	0.025	0.11
D5-1885	67.7	4.3	15.1	4.9	3.6	4.14	0.07	0.024	0.15
D5-1886	63.6	8.6	15.0	5.1	3.5	4.05	0.06	0.022	0.11
D5-1932	59.6	12.8	14.7	5.0	3.6	4.10	0.06	0.023	0.12
D5-1933	55.2	17.0	14.9	5.0	3.6	4.08	0.06	0.028	0.11

The trace chemistries are the following:

O < 10 ppm
N < 16 ppm
S < 20 ppm
Bi, Th < 0.1 ppm
Pb, Tl, Ca < 0.2 ppm

fraction of unsolutioned primary γ' inhibits grain growth as the large primary γ' precipitates tend to pin the grain boundaries. However, only a small fraction of the unsolutioned primary γ' is retained in order to maximize the amount of γ' formers available for subsequent precipitation as fine (secondary) strengthening γ'. After the partial solutioning step, the alloys were given a series of aging heat treatments to optimize the amount of secondary γ' and precipitate discrete $M_{23}C_6$ carbides at the grain boundaries.

As determined by differential thermal analysis (DTA) at SMC, the γ' solvus and solidus temperatures of the experimental alloys were found to be a function of cobalt content. Consequently, different solutioning temperatures were used in the disk heat treatment according to the γ' solvus temperature of each alloy. Table II shows the disk heat treatment schedule for each alloy including alterations in the solutioning temperatures necessary to maintain a constant grain size. The resultant average grain sizes of the alloys range from 11.0 - 13.0 μm.

To determine the effect of cobalt on the long-time microstructural stability of the experimental Udimet 700 alloys, the disk heat treated materials were given a 1000 hour aging heat treatment at 815°C (1500°F). This long-time aging (LTA) process will precipitate a sigma phase in the matrix or in the vicinity of the grain boundaries if the alloy is unstable.

3.3. Phase Extractions

The phases found in each of the experimental alloys were isolated from the matrix by three extraction techniques. Particulate residues obtained from the extractions were used for weight fraction analysis

TABLE II. Disk Heat Treatment

Solution Treatment:	
0.0, 4.3, 8.6%Co	at 1129°C (2064°F) for 4 hrs
12.8%Co	at 1118°C (2044°F) for 4 hrs
17.0%Co	at 1104°C (2019°F) for 4 hrs
Salt quench to 316°C/Air cool	
Age Treatment:	
871°C (1600°F) for 8 hrs/Air cool	
982°C (1800°F) for 4 hrs/Air cool	
649°C (1200°F) for 24 hrs/Air cool	
760°C (1400°F) for 8 hrs/Air cool	

and X-ray diffraction studies including phase identification, lattice parameter measurements and a semiquantitative analysis of the amount of each phase present in the experimental alloys. In addition the extracted residues were used to study the morphology and chemical composition of each isolated phase using a Scanning Electron Microscope (SEM) and energy dispersive X-ray analyzer.

3.3.1. Electrolytic Extraction of Carbides, Borides and Sigma: Extraction Technique EX-1

The carbide, boride, and sigma phases were isolated from the γ matrix and γ' by a standard electrolytic extraction technique using a 10% Hydrochloric Acid-Methanol Electrolyte.[30,31] Because of excessive matrix contamination encountered during the standard four hour extraction period, the extraction time was reduced to two hours and the current densities were adjusted for each cobalt level. Figure 1 shows the current densities used to extract the experimental alloys as a function of cobalt content. A detailed review of the procedures concerning sample preparation, the EX-1 extraction technique,and the determination of the wt.% of extracted residue are found in Sections 1 and 2 of the Appendix.

3.3.2. Chemical Extraction of Carbides and Borides: Extraction Technique EX-2

The carbide and boride phases were chemically isolated from the γ matrix, γ',and sigma phases via chemical dissolution in a 10% Bromine-Methanol reagent. Normally, the grain boundary type $M_{23}C_6$ carbides which form during heat treatment or engine exposure in many nickel-base

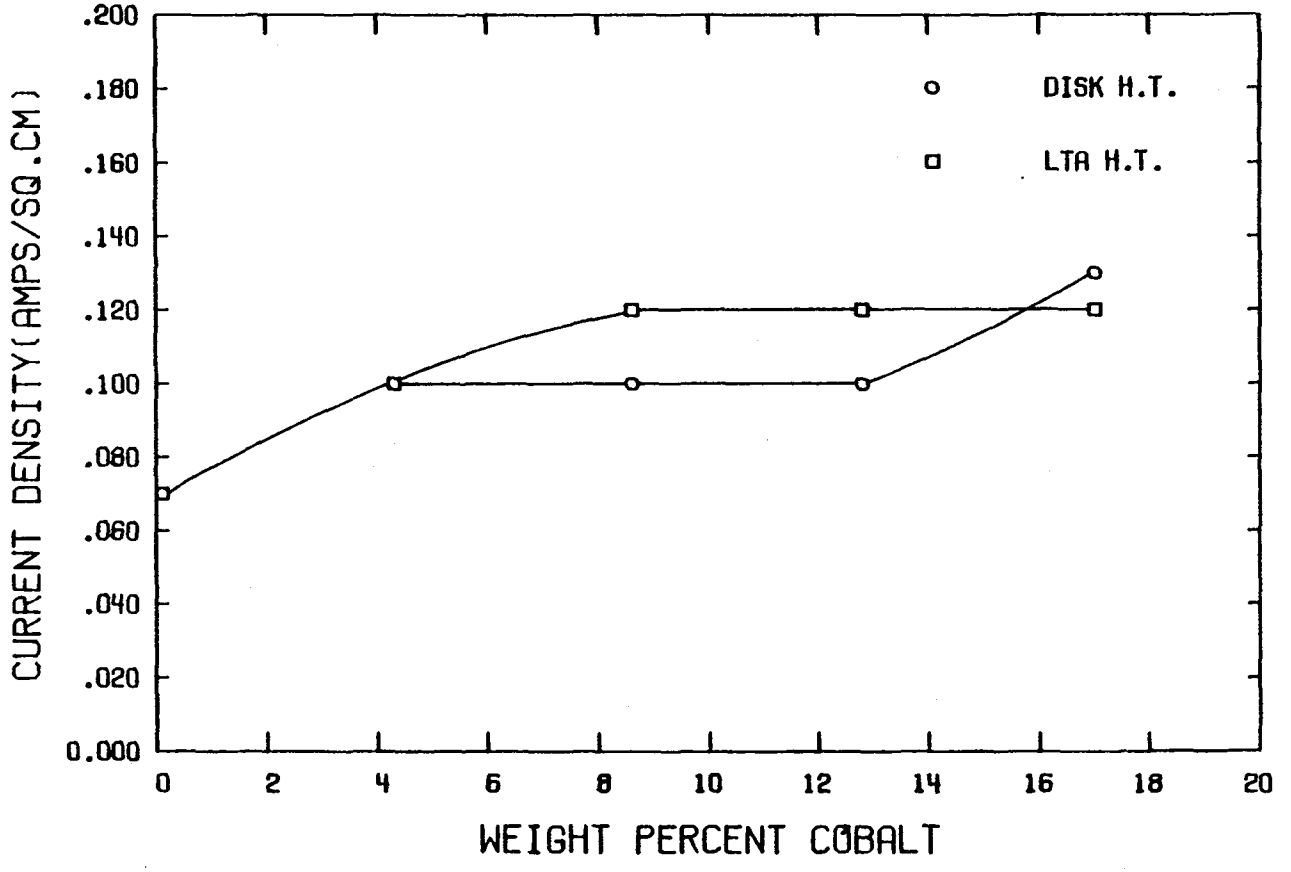

FIGURE 1. CURRENT DENSITIES OF EX-1(HCL) EXTRACTIONS VS. WEIGHT PERCENT COBALT

superalloys are dissolved in this EX-2 extraction. However, other types of $M_{23}C_6$ carbides which may form during processing may be isolated by this extraction technique. A detailed description of the EX-2 extraction procedure is found in Section 3 of the Appendix.

3.3.3. Electrolytic Extraction of Gamma Prime (γ')

The γ' phases were electrolytically extracted from the γ matrix in an electrolyte consisting of 1% Ammonium Sulfate and 1% Citric Acid (by weight) in deionized water.[31,32] However, a minor amount of the phases normally extracted in the EX-1 type extraction technique are also extracted by this method. A current density of 0.03 Amp/cm^2 was maintained throughout the three hour room temperature extraction. A detailed explanation of the γ' extraction procedure and the determination of the wt.% of extracted γ' is found in Section 4 of the Appendix.

3.4. X-Ray Diffraction Studies

3.4.1. Analysis of the Residues From the EX-1 and EX-2 Extraction Techniques

The EX-1 and EX-2 extracted residues were subjected to X-ray powder diffraction analysis to identify the phases present, their relative intensities,and crystal structures. The relative intensities of the primary (hkl) peaks of the phases found in the extracted residues were used as a semiquantitative measure of the amount of each phase present in the experimental alloys.

A General Electric (GE) X-ray diffractometer was used to produce the diffraction patterns using nickel filtered CuK_α radiation. A 1° primary beam slit and a 0.2° detector slit were used. Although the

GE diffractometer is more than adequate for phase identification and X-ray peak intensity measurements, its accuracy is limited to approximately $\pm$ 0.01 Å, and therefore inadequate for precise lattice parameter measurements.

3.4.2. Lattice Parameter Studies

Lattice parameters of the γ matrix as well as the primary (coarse) and secondary (fine) extracted γ' phases were calculated using a modified version of the LCR-2 Lattice Constant Refinement computer program which was developed by Williams.[33] This program uses a weighted least squares method to calculate the lattice parameter from the measured diffraction peak locations. Four extrapolation functions are used in the LCR-2 program to correct for systematic experimental errors. The locations of the diffraction peak maxima were accurately determined using a computerized five (2θ intensity) point parabola fitting program. This program was used in an iterative manner to locate the I_{max} of each (hkl) diffraction peak.

An automated Siemens powder X-ray diffractometer was used to produce the X-ray diffraction patterns. X-rays were generated from a cobalt X-ray tube operated at 40 kV and 20 mA. A 2° primary beam slit and a 1/4° detector slit were used.

The coarse and fine γ' particles, which had been isolated by a separation technique described in Section 5 of the Appendix, were subjected to monochromated CoK_{α} radiation. However, it was necessary to use monochromated CoK_{β} radiation for analysis of the γ matrix samples due to complications caused by partial overlapping of the K_{α_1} and K_{α_2} peaks. The following (hkl) peaks were used to determine the

calculated lattice parameters of the γ matrix and extracted γ' (residue):

(hkl)	γ' Residue	γ Matrix
111	K_α Average	K_β
200	K_α Average	K_β
220	K_{α_1}	K_β
311	K_{α_1} and K_{α_2}	K_β
222	K_{α_1} and K_{α_2}	

The solid alloy samples used to determine the lattice parameters of the matrix were electropolished and immersion etched as described in Section 3.5.1.

3.5. Scanning Electron Microscopy

3.5.1. Sample Preparation

In preparation for microstructural analysis, samples of the experimental alloys were wet ground through a 600 grit silicon carbide abrasive and subsequently electropolished in a 20% Sulfuric Acid-Methanol solution. A stainless steel beaker containing the electrolyte functioned as a cathode while a potential of 20 volts was applied for a 10 sec electropolishing period. Each specimen was then immersion etched for 20 sec in a 15% Hydrochloric Acid-Methonal solution to which a few drops of Hydrogen Peroxide had been added immediately prior to etching. This procedure enhances the microstructural contrast of the samples by etching out the γ' precipitates, leaving the carbide, boride, and any TCP phases in relief.

3.5.2. Microstructural and Chemical Analysis

After optical metallographic studies, a Japan Electron Optics Laboratories (JEOL) JSM-U3 Scanning Electron Microscope (SEM) was used to study the microstructure of the experimental alloys and extracted residues. An Energy Dispersive X-ray Analyzer (EDAX) 9100 system attached to the SEM was used to obtain qualitative and quantitative chemical analyses of the phases present in the alloy samples and extracted residues. Analyses of the phases in situ were complicated due to excitation of elements from the adjacent γ matrix; therefore, extracted particles (no matrix) were chemically analyzed.

IV. RESULTS

4.1. Scanning Electron Microscopy

4.1.1. Disk Heat Treated Microstructure

Figures 2 and 3 represent the disk heat treated microstructure of the modified Udimet 700 alloys containing 0.1, 8.6, and 17.0 wt.% cobalt. The dark blocky regions are γ' particles which have been etched out of the matrix. Two distinct sizes of γ' are observed in Fig. 3(a), (b), and (c). The coarse-primary or unsolutioned γ' is frequently seen pinning the grain boundaries and the fine-secondary or strengthening γ' is found dispersed throughout the γ matrix. Titanium rich MC carbides and molybdenum rich M_3B_2 borides are observed in both transgranular and grain boundary locations. In addition, fine-discrete chromium rich $M_{23}C_6$ carbides are found decorating the grain boundaries. However, the low cobalt alloys contain an abundance of massive chromium rich $M_{23}C_6$ carbides (large, bright particles) often surrounded by or adjacent to unsolutioned primary γ' and frequently occurring in clusters, as shown in Fig.3(a). When observed longitudinally to the rolling direction, these clusters appear as stringers of the massive $M_{23}C_6$ carbides as seen in Figs. 4 and 5.

It is evident that cobalt has a significant affect upon the microstructure of these experiment alloys of Udimet 700 in the disk heat treated condition. As cobalt is reduced, the size and weight

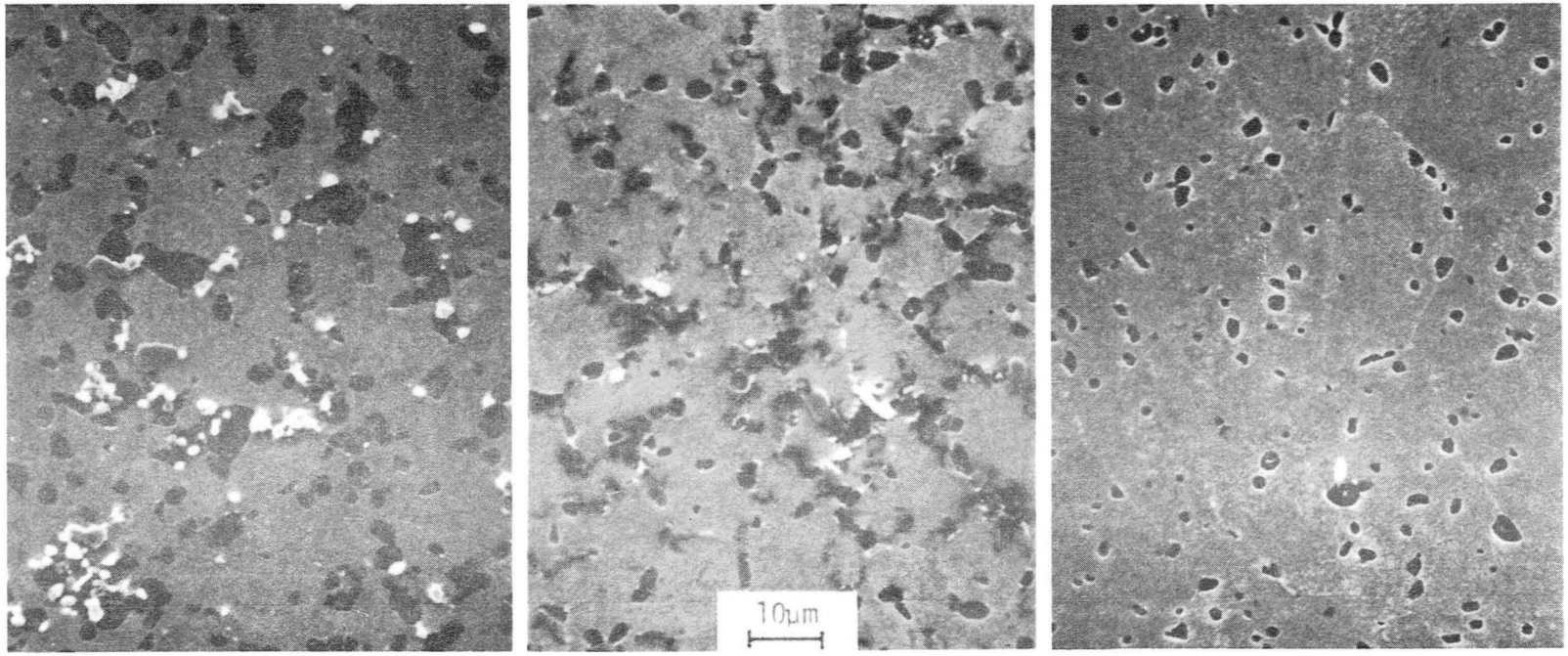

(a) 0.1 wt.%Co (b) 8.6 wt.%Co (c) 17.0 wt.%Co

Figure 2. SEM Micrographs of Disk Material; (a) 0.1 wt.%Co, (b) 8.6 wt.%Co, (c) 17.0 wt.%Co. (1000X)

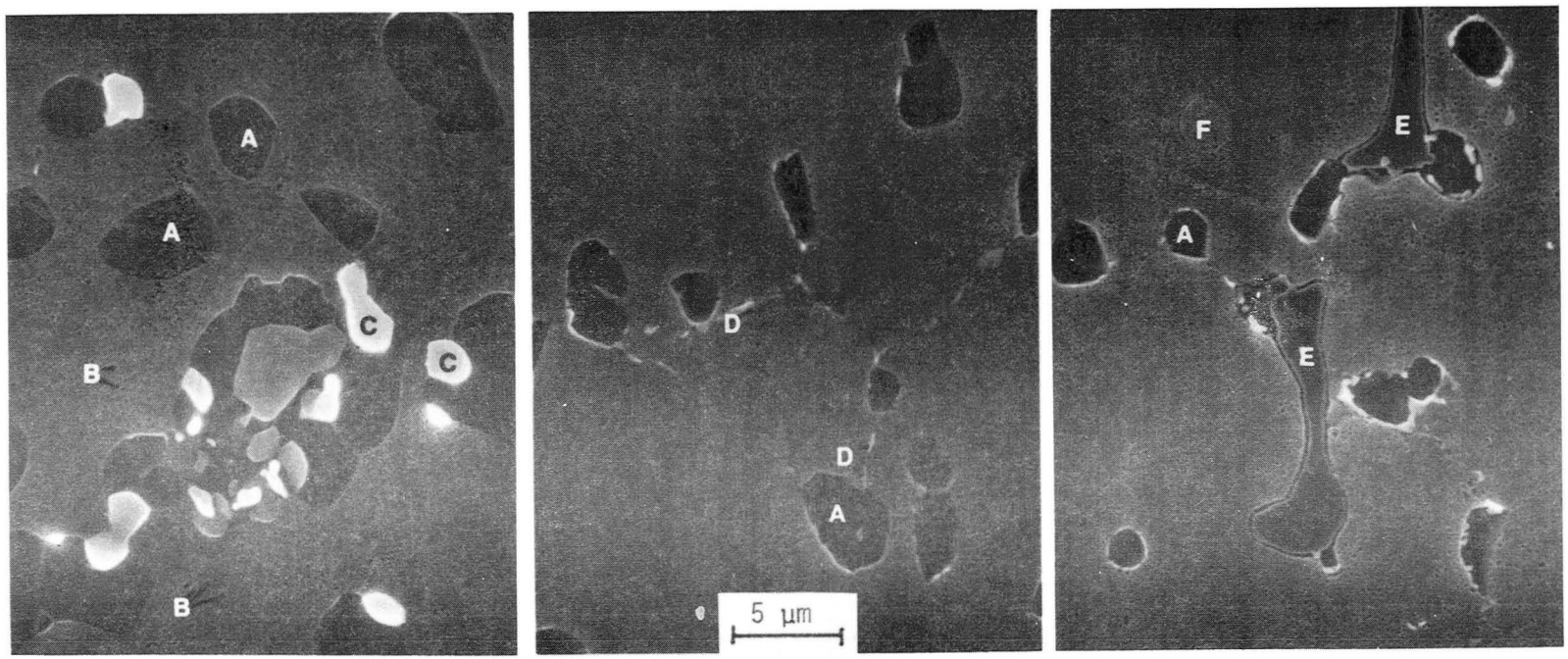

(a) 0.1 wt.%Co (b) 8.6 wt.%Co (c) 17.0 wt.%Co

Figure 3. SEM Micrographs of Disk Material; (a) 0.1 wt.%Co, (b) 8.6 wt.%Co, (c) 17.0 wt.%Co. (3000X)
[A-Primary γ', B-Secondary γ', C-Massive $M_{23}C_6$ Carbide, D-Grain Boundary $M_{23}C_6$ Carbide, E-MC Carbide, and F-M_3B_2]

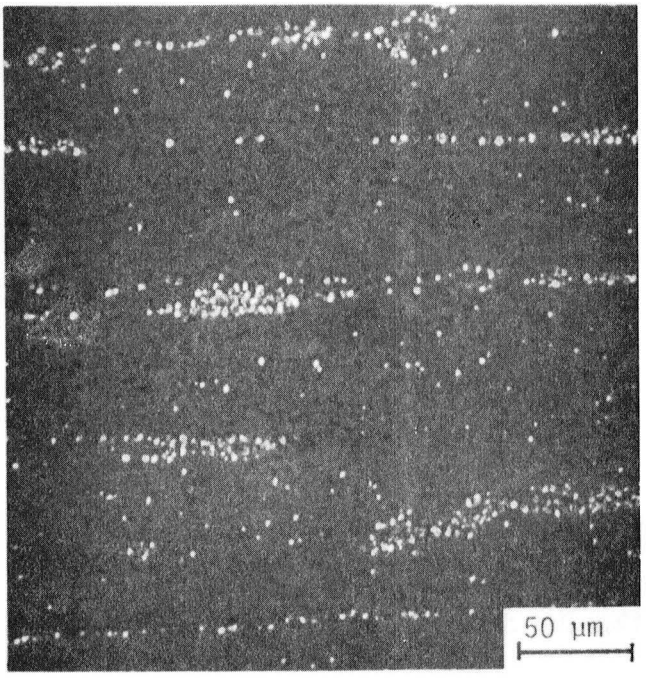

Figure 4. SEM Micrograph of Massive $M_{23}C_6$ Carbide Stringers in the 0.1 wt.%Co Disk Material. (300X)

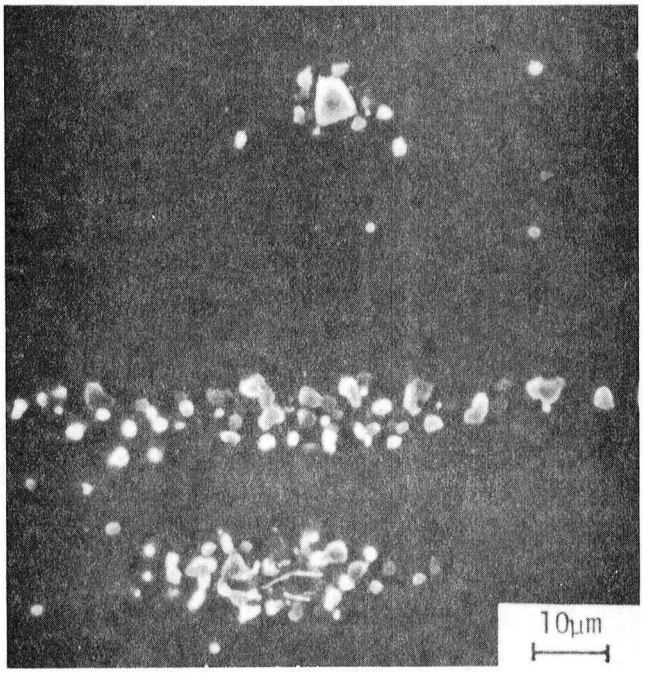

Figure 5. SEM Micrograph of Massive $M_{23}C_6$ Carbide Stringers in the 0.1 wt.%Co Disk Material. (1000X)

fraction of unsolutioned primary γ' is observed to increase (Fig. 3(a), (b), and (c). Precipitation of the grain boundary $M_{23}C_6$ carbides initially increases as cobalt is decreased to 12.8 and 8.6 wt.% cobalt. At 8.6 wt.% cobalt the first of the massive $M_{23}C_6$ carbides begin to form, subsequently becoming the dominant carbide phase in the lower cobalt alloys. The formation of the titanium rich MC carbides is also observed to be relatively sensitive to cobalt content. As cobalt is reduced, the amount of MC carbide formation decreases until very few are found in the cobalt-free alloy (< 0.1 wt.% cobalt). Although few in number, the molybdenum rich M_3B_2 borides appear to be least affected by cobalt content in the disk heat treated alloys.

4.1.2 LTA Heat Treated Microstructure

Figures 6 through 7 represent the microstructure of the modified Udimet 700 alloys containing 0.1, 8.6, and 17.0 wt.% cobalt, following a long time age (LTA) heat treatment. These alloy samples, which were initially disk heat treated prior to the LTA cycle at 815°C (1500°F) for 1000 hours,exhibit an increase in the size and volume fraction of the fine strengthening γ' precipitates. Furthermore, the precipitation of discrete grain boundary $M_{23}C_6$ carbides increases in all of the alloys aside from the cobalt free version. Clusters of the massive $M_{23}C_6$ carbides were again noted in the lower cobalt alloys (< 0.1 and 4.3 wt.%) as seen in Fig. 6(a).

An additional consequence of the LTA heat treatment was the formation of a sigma phase in the vicinity of the grain boundaries, which was first observed in the 8.6 wt.% cobalt alloy (Fig.7(b)). The amount of sigma increased significantly in the 12.8 and 17.0 wt.% cobalt alloys (Fig.7(b,c)).

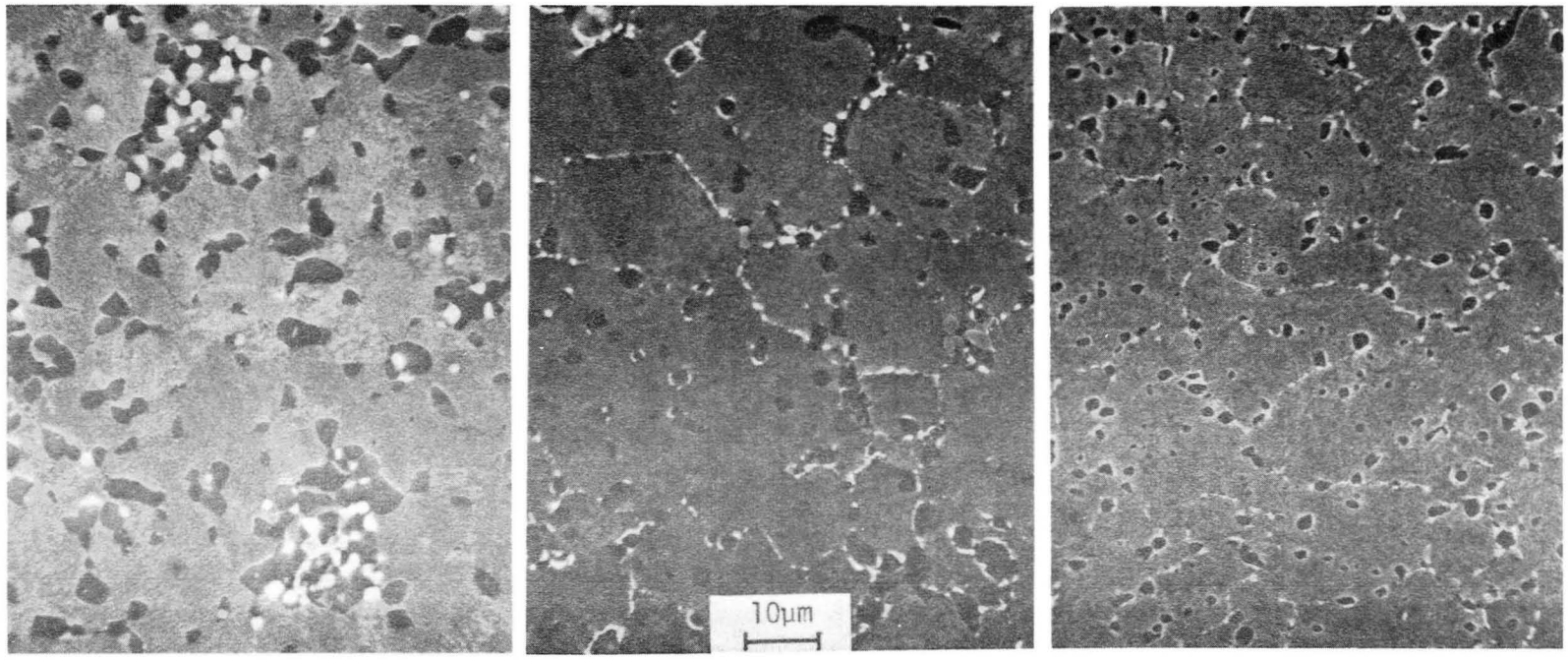

(a) 0.1 wt.%Co (b) 8.6 wt.% Co (c) 17.0 wt.%Co

Figure 6. SEM Micrographs of LTA Material; (a) 0.1 wt.%Co, (b) 8.6 wt.%Co, (c) 17.0 wt.%Co. (1000X)

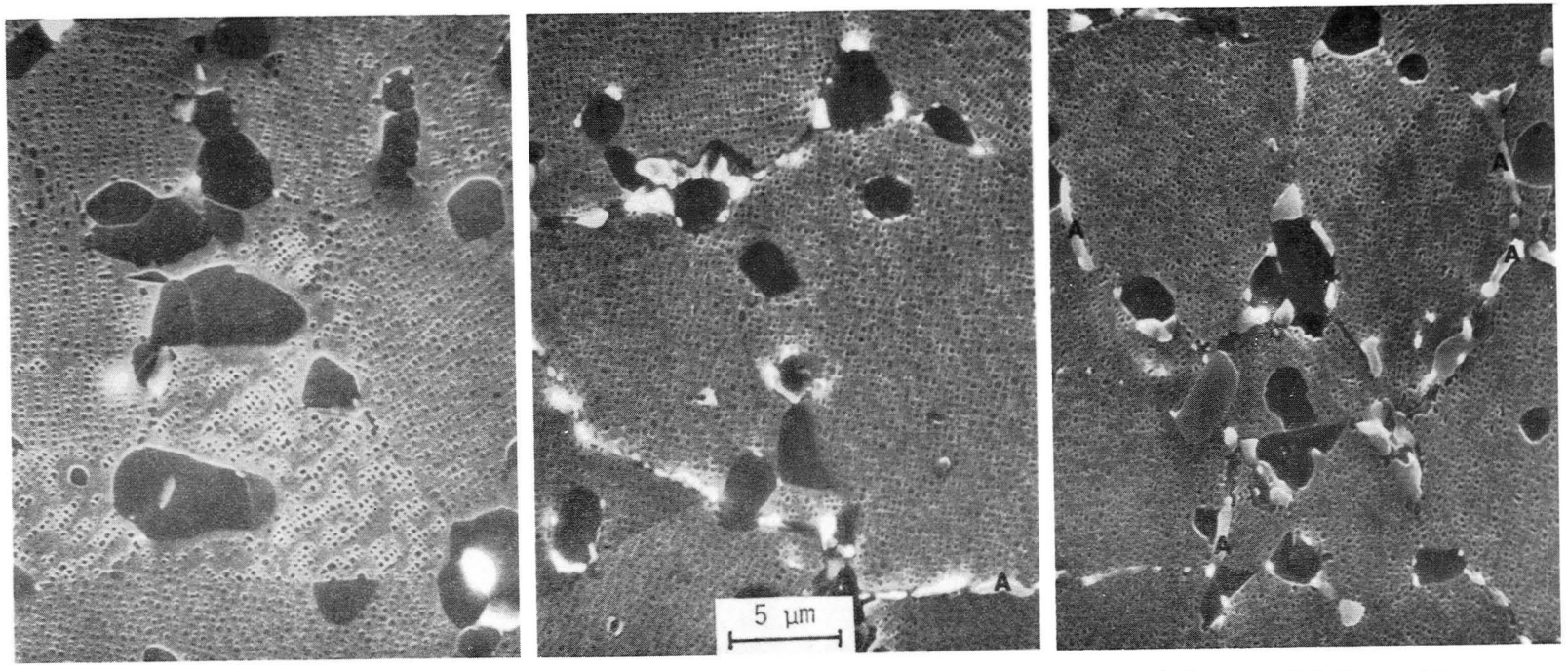

(a) 0.1 wt.%Co (b) 8.6 wt.%Co (c) 17.0 wt.%Co

Figure 7. SEM Micrographs of LTA Material; (a) 0.1 wt.%Co, (b) 8.6 wt.%Co, (c) 17.0 wt.%Co. (3000X)
[A-Sigma Phase]

4.1.3. EDAX Analysis of Phases

Energy Dispersive Analysis of X-rays (EDAX) was used to analyze the phases found in the extracted residues from the modified Udimet 700 alloys. The resultant average chemistries were determined through a standardless EDAX analysis of each particulate phase as follows:

1. Titanium rich MC type carbide

   $(Ti_{.65}Mo_{.25}Cr_{.10})C$

2. Chromium rich $M_{23}C_6$ carbide

   (a) Grain boundary $M_{23}C_6$ carbide

   $(Cr_{.77}Mo_{.14}Ni_{.08}Ti_{.01})_{23}\ C_6$

   (b) Massive $M_{23}C_6$ carbide

   $(Cr_{.67}Mo_{.24}Ni_{.05}Ti_{.01})_{23}\ C_6$

3. Molybdenum rich M_3B_2 type boride

   $(Mo_{.72}Cr_{.25}Ni_{.02}Ti_{.01})_3\ B_2$

4. Gamma Prime (γ')

   $Ni_3(\underline{Al},\underline{Ti},Cr,Mo,Co)$

5. Sigma*

   Ni-Cr-Co-Mo

   *(Found only in the LTA heat treated 8.6, 12.8, and 17.0 wt.% cobalt alloys.)

Note that the massive type of $M_{23}C_6$ carbide found only in the low cobalt alloys contains more molybdenum and less chromium than the fine-grain boundary carbides. EDAX analysis was also used to study the effect of alloy cobalt content on cobalt partitioning into the aforementioned phases. The amount of cobalt found in each of these

phases was observed to increase with increased cobalt content in the experimental alloys.

4.2. Phase Extraction Study

4.2.1. EX-1 (Hydrochloric-Methanol) Extraction

This electrolytic extraction technique dissolves the γ' and γ matrix, thereby isolating the MC, $M_{23}C_6$, M_3B_2 and/or sigma phases found in these experimental alloys. Figure 8 shows the effect of cobalt content on the wt.% of extracted residue of the disk and LTA heat treated alloys, which is also listed in Table III. Note that the quantities of residue extracted from the low cobalt alloys, which are dominated by the massive $M_{23}C_6$ carbide, are relatively constant. The amount of residue extracted from the disk heat treated material decreases with increasing cobalt, as the massive $M_{23}C_6$ carbide phase is eliminated from the higher cobalt alloys. However, the amount of residue extracted from the LTA heat treated alloys increases significantly as cobalt increases from 8.6 to 17.0 wt.% cobalt, which is primarily due to the formation of large quantities of the sigma phase and additional precipitation of grain boundary $M_{23}C_6$ carbide phase.

4.2.2. EX-2 (Bromine-Methanol) Extraction

This chemical extraction technique isolates the MC, M_3B_2 and large blocky $M_{23}C_6$ phases while dissolving the γ', γ matrix, fine-grain boundary $M_{23}C_6$ carbides and/or sigma phases found in these experimental alloys. Figure 9 and Table III show the wt.% of extracted residue as a function of cobalt content in the disk and LTA heat treated alloys. The larger amounts of extracted residue from the low cobalt disk heat

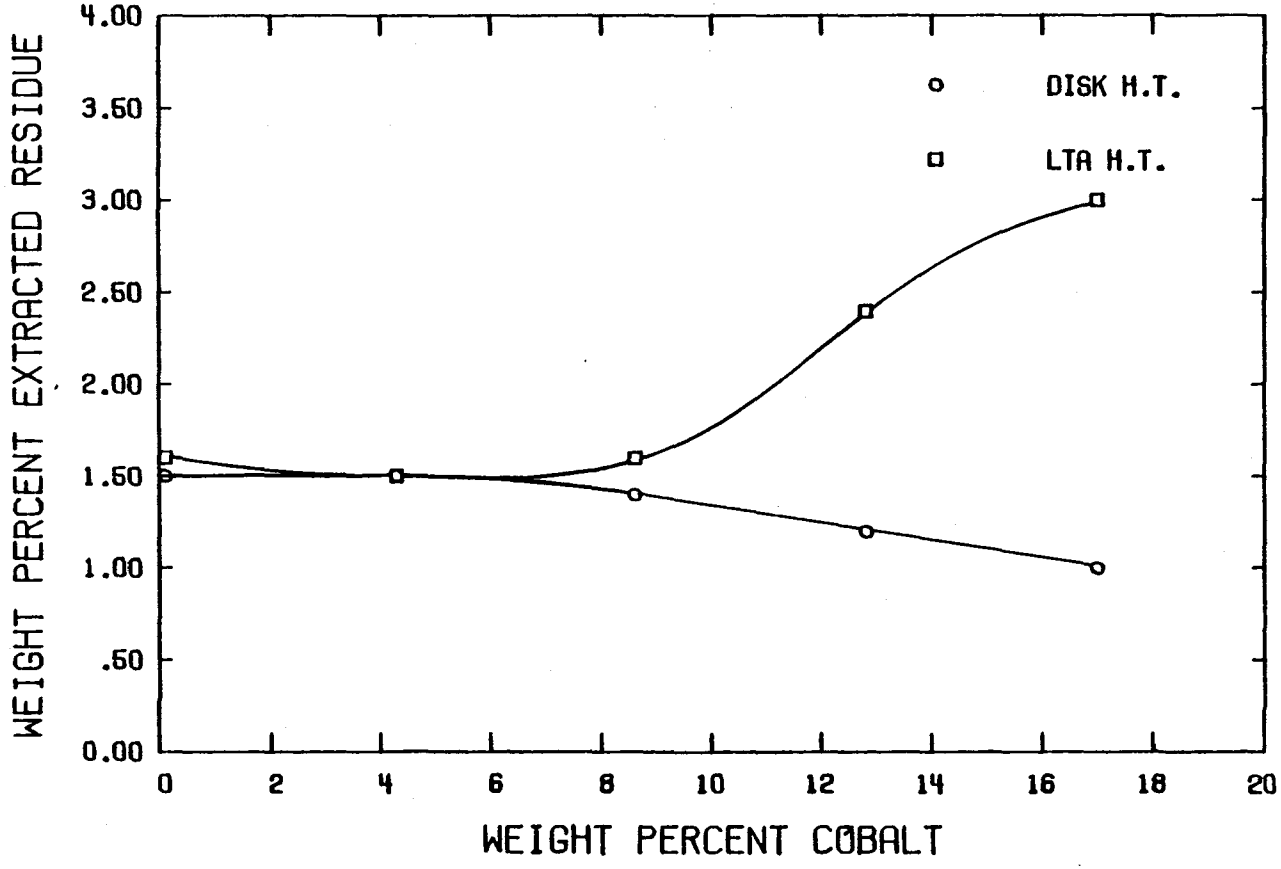

FIGURE 8. WEIGHT PERCENT EX-1(HCL) RESIDUE IN U-700 DISK AND LTA MATERIAL

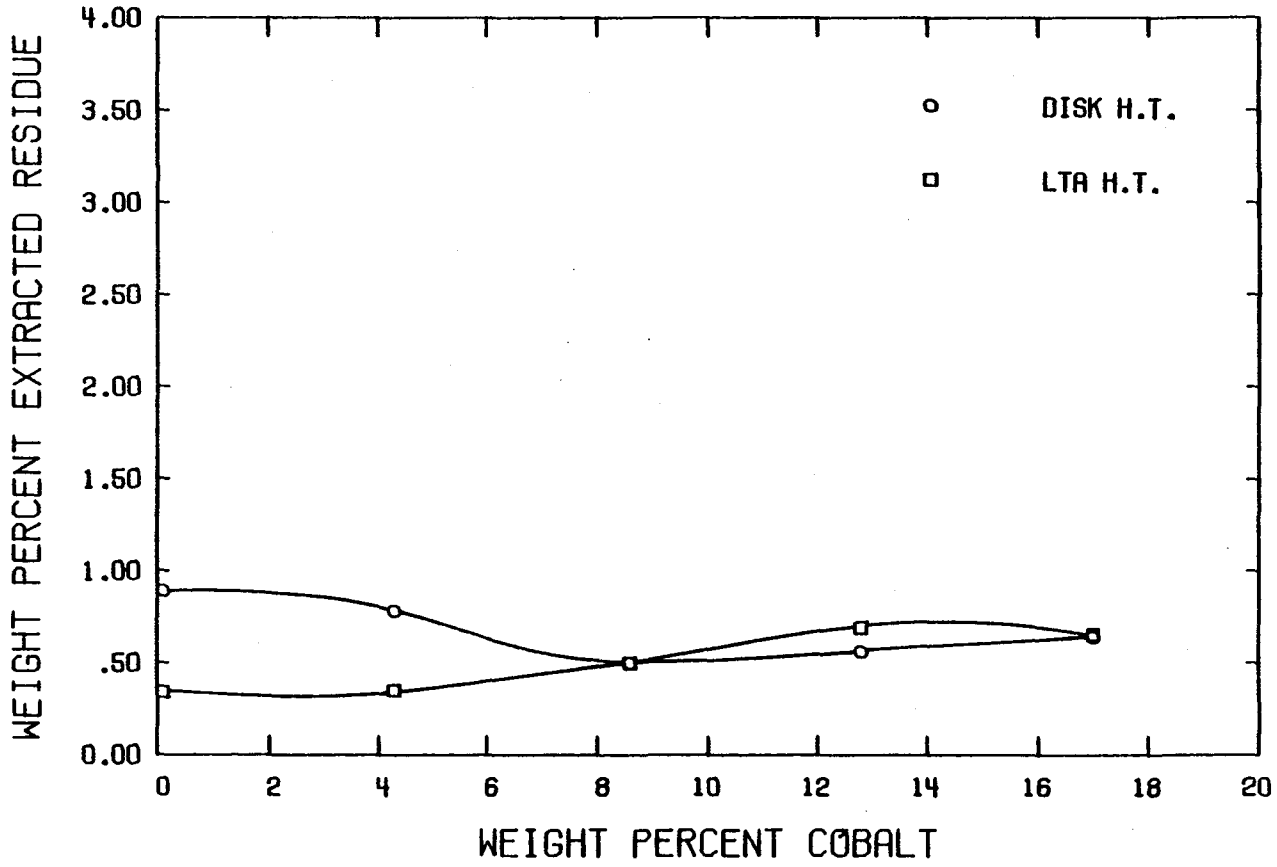

FIGURE 9. WEIGHT PERCENT EX-2(BR) RESIDUE IN U-700 DISK AND LTA MATERIAL

TABLE III. Weight Percent of Extracted Residues

Wt.% Co.	Wt.% EX-1 Residue	
	Disk. H.T.	LTA H.T.
0.1	1.5	1.6
4.3	1.5	1.5
8.6	1.4	1.6
12.8	1.2	2.4
17.0	1.0	3.0
Wt.% Co	Wt.% EX-2 Residue	
	Disk. H.T.	LTA H.T.
0.1	0.89	0.34
4.3	0.78	0.35
8.6	0.50	0.50
12.8	0.56	0.69
17.0	0.64	0.65
Wt. % Co	Wt.% Gamma Prime	
	Disk H.T.	LTA H.T.
0.1	45.8	46.7
4.3	45.9	47.0
8.6	46.0	46.9
12.8	46.8	45.9
17.0	46.0	44.3

treated material is due to the increased quantities of the massive $M_{23}C_6$ carbides present. As cobalt is added, the amount of extracted residue initially decreases to a minimum at 8.6 wt.% cobalt, whereupon the MC and M_3B_2 phases become more prevalent with increased precipitation in the higher cobalt alloys.

In the LTA heat treated alloys, the massive $M_{23}C_6$ carbides become less resistant to dissolution as indicated by the smaller amounts of extracted residue in the lower cobalt alloys. The increased quantities of extracted residue noted in the higher cobalt alloys are a result of increased formation of the MC and M_3B_2 phases.

4.2.3. Gamma Prime (γ') Extraction

This electrolytic extraxction technique primarily isolates the γ' along with a minor fraction of the EX-1 type residues which is subtracted from the overall extraction to obtain the corrected percentage of γ' as shown in previous work.[21] Figure 10 and Table III show the wt.% of γ' as a function of cobalt content in the experimental alloys. In the disk heat treated alloys, the amount of γ' remains fairly constant aside from a maximum noted at 12.8 wt.% cobalt. An increased amount of γ' is noted in the LTA heat treated alloys containing 0.1, 4.3 and 8.6 wt.% cobalt, as aging at 815°C (1500°F) enhances the formation of fine-strengthening γ' precipitates. Cobalt is seen to have little effect upon the amount of γ' found in the LTA heat treated alloys containing 0.1, 4.3, and 8.6 wt.% cobalt. However, the amount of γ' in the 12.8 and 17.0 wt.% cobalt alloys decreases because of the large quantities of sigma present in these experimental alloys.

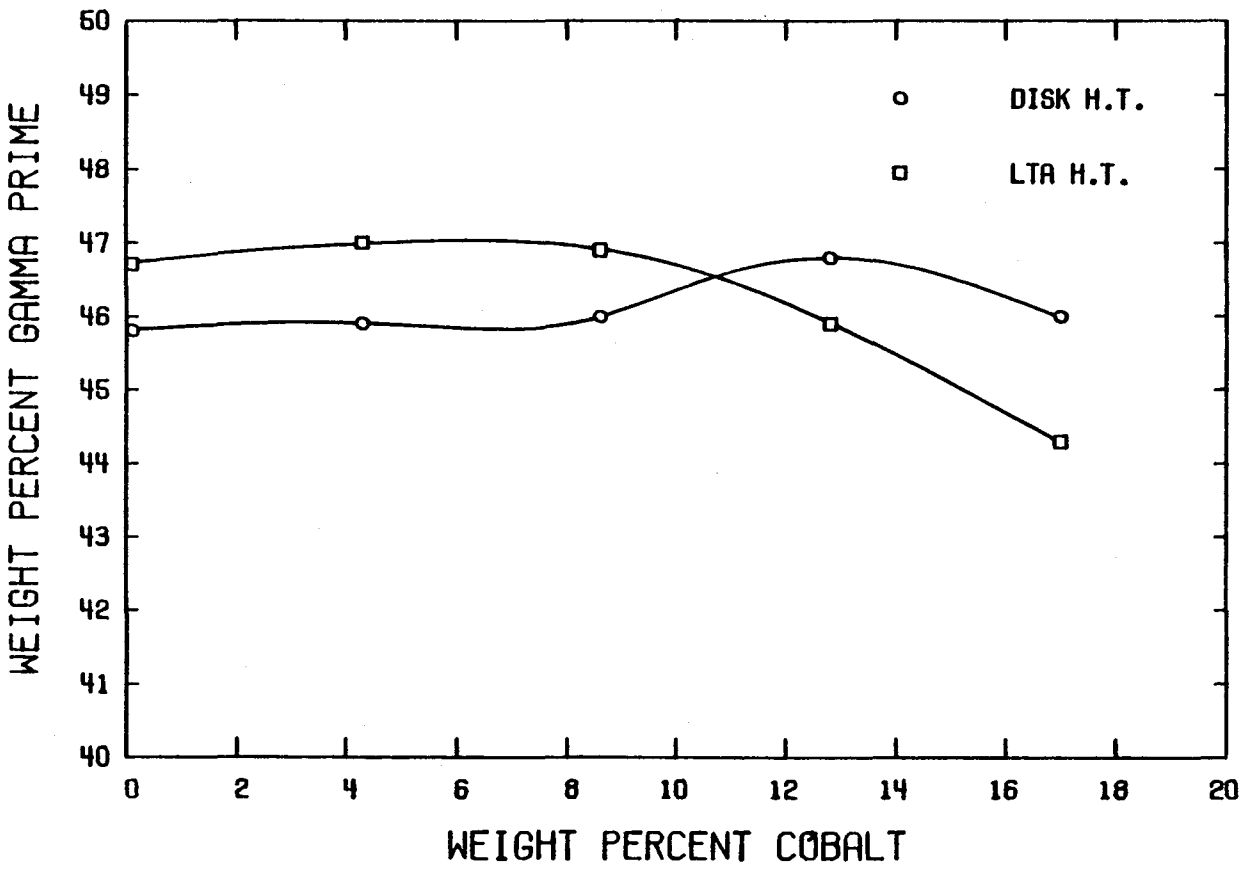

FIGURE 10. WEIGHT PERCENT GAMMA PRIME IN U-700 DISK AND LTA MATERIAL

4.3. X-Ray Diffraction Analysis of the Minor Phases

4.3.1. Residue Analysis

X-ray diffraction (XRD) techniques were used to determine the relative amounts of the minor phases such as the MC, $M_{23}C_6$, M_3B_2 and/or sigma phases present in each of the experimental alloys. These results were derived from a comparative study of the relative intensities of the diffraction peaks from each of the minor phases found in the extracted residues. Accordingly, the relative XRD peak intensities are a semi-quantitative measure of the amount of minor phases found in the experimental alloys.

4.3.2. Analysis of the EX-1 Extracted Residue

Figures 11 and 12 graphically present the effect of cobalt content on the relative amount of each minor phase found in the disk and LTA heat treated alloys, respectively. In both cases the extracted residues from the low cobalt alloys are dominated by the massive $M_{23}C_6$ carbide phase which diminishes as cobalt is added, while the amounts of the MC and M_3B_2 phases increase. However, in the higher cobalt LTA heat treated alloys the relative amounts of the MC and M_3B_2 phase appear to be "artificially" reduced as a result of the large quantities of sigma present in these alloys. It is apparent that the abundance of sigma in the extracted residue tends to "bury" the MC and M_3B_2 particles, which in turn distorts the relative XRD intensities of these phases. The result is a strong sigma XRD peak and very weak MC and M_3B_2 peaks. This was verified by metallographic analysis and through the analysis of the EX-2 type residues which will be explained in the following section.

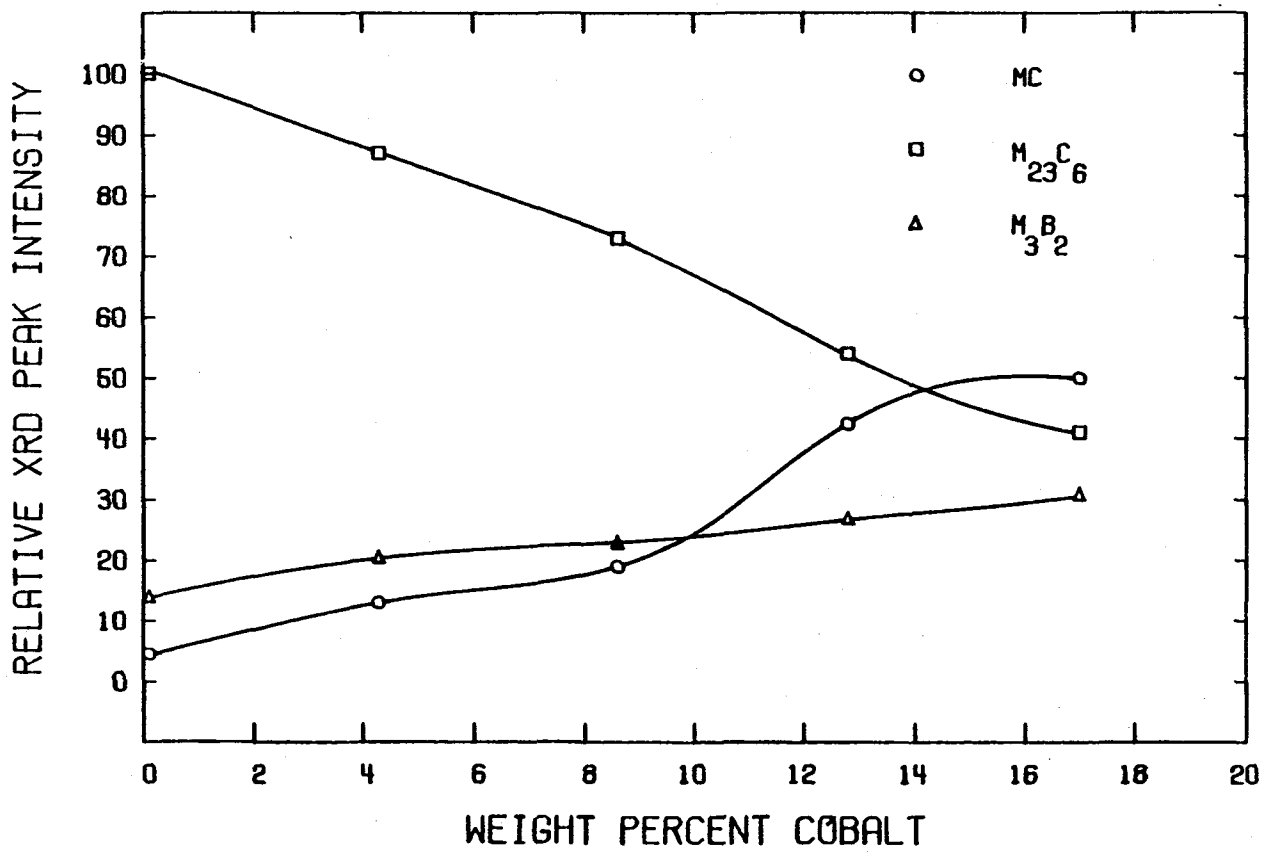

FIGURE 11. RELATIVE XRD PEAK INTENSITIES OF U-700 DISK EX-1(HCL) EXTRACTED RESIDUES

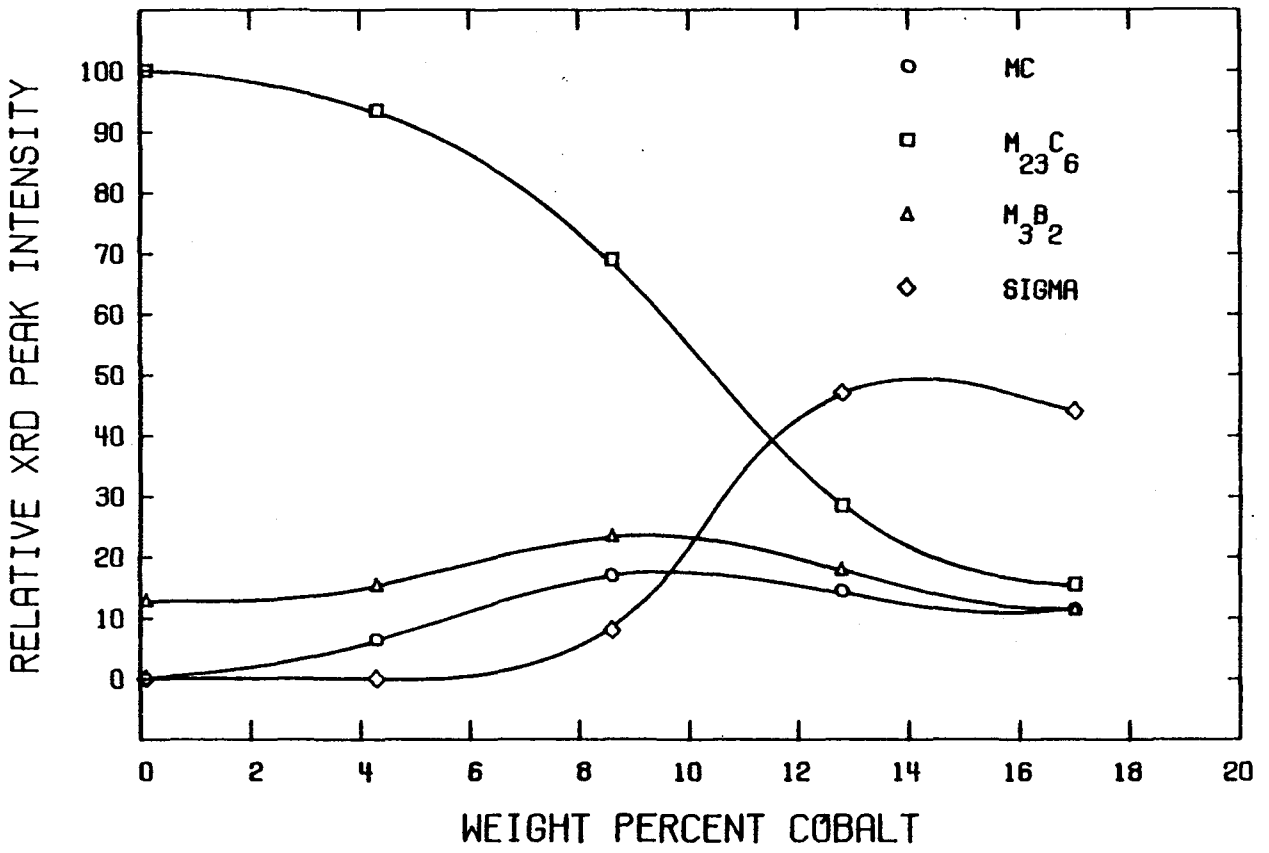

FIGURE 12. RELATIVE XRD PEAK INTENSITIES OF U-700 LTA EX-1(HCL) EXTRACTED RESIDUES

4.3.3. Analysis of the EX-2 Extracted Residue

Figures 13 and 14 depict the effect of cobalt on the relative quantities of the MC, massive $M_{23}C_6$ and M_3B_2 phases present in the disk and LTA heat treated alloys, respectively. The EX-2 type residue is devoid of the grain boundary $M_{23}C_6$ carbide and sigma phases. The massive $M_{23}C_6$ carbide is again shown to dominate the residue extracted from the low cobalt alloys and is seen to be quite sensitive to cobalt content in both the disk and LTA heat treated alloys. As cobalt is added the amount of these massive $M_{23}C_6$ carbides significantly decreases until they are nonexistent in the 12.8 and 17.0 wt.% cobalt alloys. Furthermore, the massive $M_{23}C_6$ carbides found in the low cobalt (0.1 and 4.3 wt.% cobalt) LTA heat treated alloys are observed to be much less resistant to dissolution in the bromine solution than those found in the disk heat treated alloys.

The amount of MC carbide is observed to increase with increasing cobalt, most prominently in the higher cobalt alloys, both in the disk and LTA heat treated condition. In addition, the relative quantity of the M_3B_2 boride increases with increasing cobalt in the LTA heat treated alloy and changes very little in the disk heat treated material. The significant increases in the amounts of the MC and M_3B_2 phases present in the higher cobalt versions of the LTA heat treated alloys are quite evident in the absence of the sigma phase in the EX-2 type residue. Also note that the MC is the predominate phase in the extracted residues from the higher cobalt containing alloys in both the disk and LTA condition.

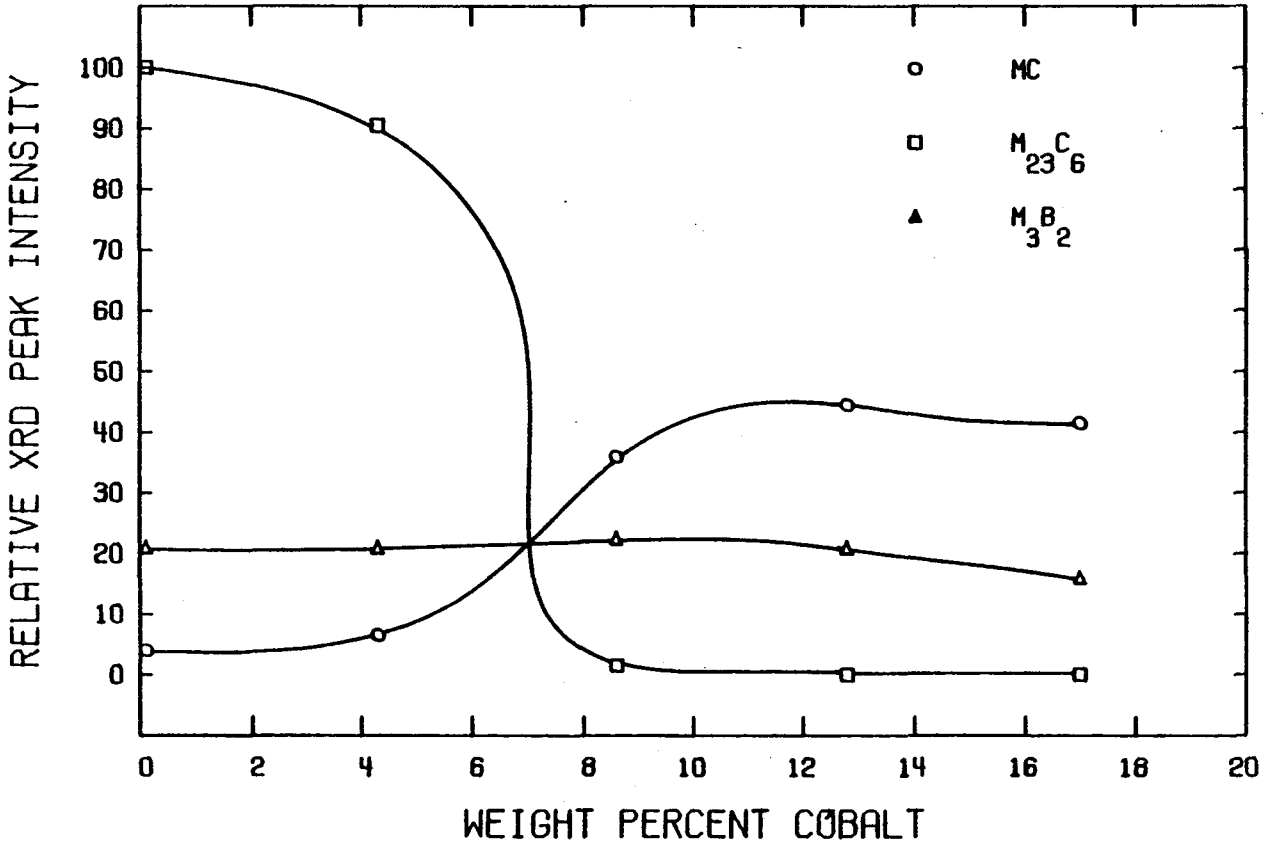

FIGURE 13. RELATIVE XRD PEAK INTENSITIES OF U-700 DISK EX-2(BR) EXTRACTED RESIDUES

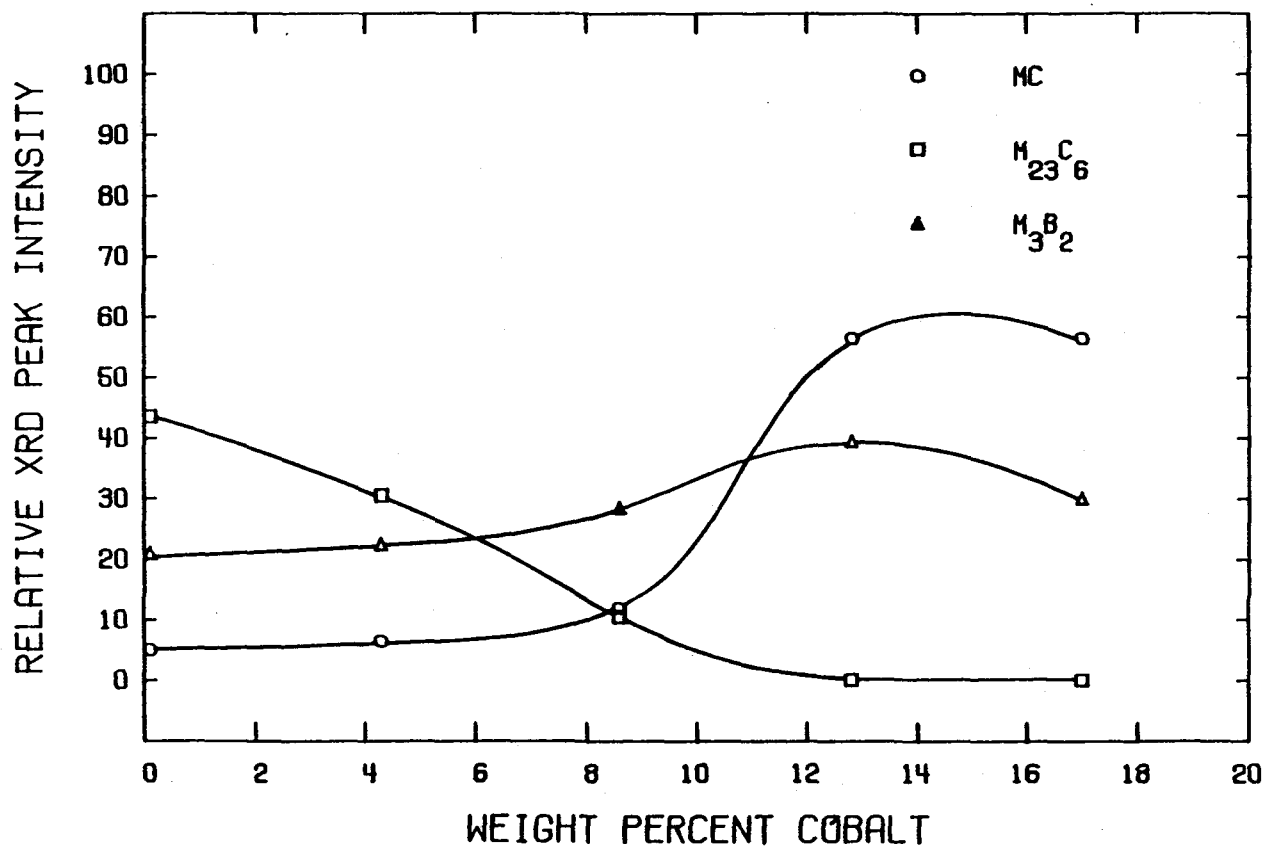

FIGURE 14. RELATIVE XRD PEAK INTENSITIES OF U-700 LTA EX-2(BR) EXTRACTED RESIDUES

4.4. Lattice Parameter Study

4.4.1. Precision Lattice Parameter Measurement of the Gamma Prime (γ')

The lattice parameters and estimated standard deviation (ESD) of the primary (coarse) and secondary (fine) γ' in the disk and LTA heat treated alloys are shown in Figs. 15 and 16, respectively. This data is also listed numerically in Table IV. In both the disk and LTA heat treated alloys, the lattice parameters of the coarse and fine γ' are observed to increase slightly with increasing cobalt content. The lattice parameters of the coarse γ' are found to be consistently larger than those of the fine γ' in every case.

4.4.2. Precision Lattice Parameter Measurement of the Gamma Matrix (γ)

Figure 17 and Table IV show the lattice parameters and estimated standard deviation (ESD) of the γ matrix in the disk and LTA heat treated alloys. The γ lattice parameter of the disk heat treated alloys increases with increasing cobalt content, much more than the lattice parameter increase noted in the LTA heat treated samples. In both the disk and LTA heat treated alloys, the most substantial lattice parameter increase was noted as the cobalt content is increased from 0.1 to 4.3 wt.%.

4.4.3. Gamma Matrix (γ) and Gamma Prime (γ') Lattice Mismatch

The lattice mismatch between austenitic γ matrix and age-hardening γ' precipitate was calculated using the following equation:[34]

$$\text{percent mismatch} = \frac{a_o \text{ matrix } (\gamma) - a_o \text{ precipitate } (\gamma')}{a_o \text{ matrix } (\gamma)} \times 100\%$$

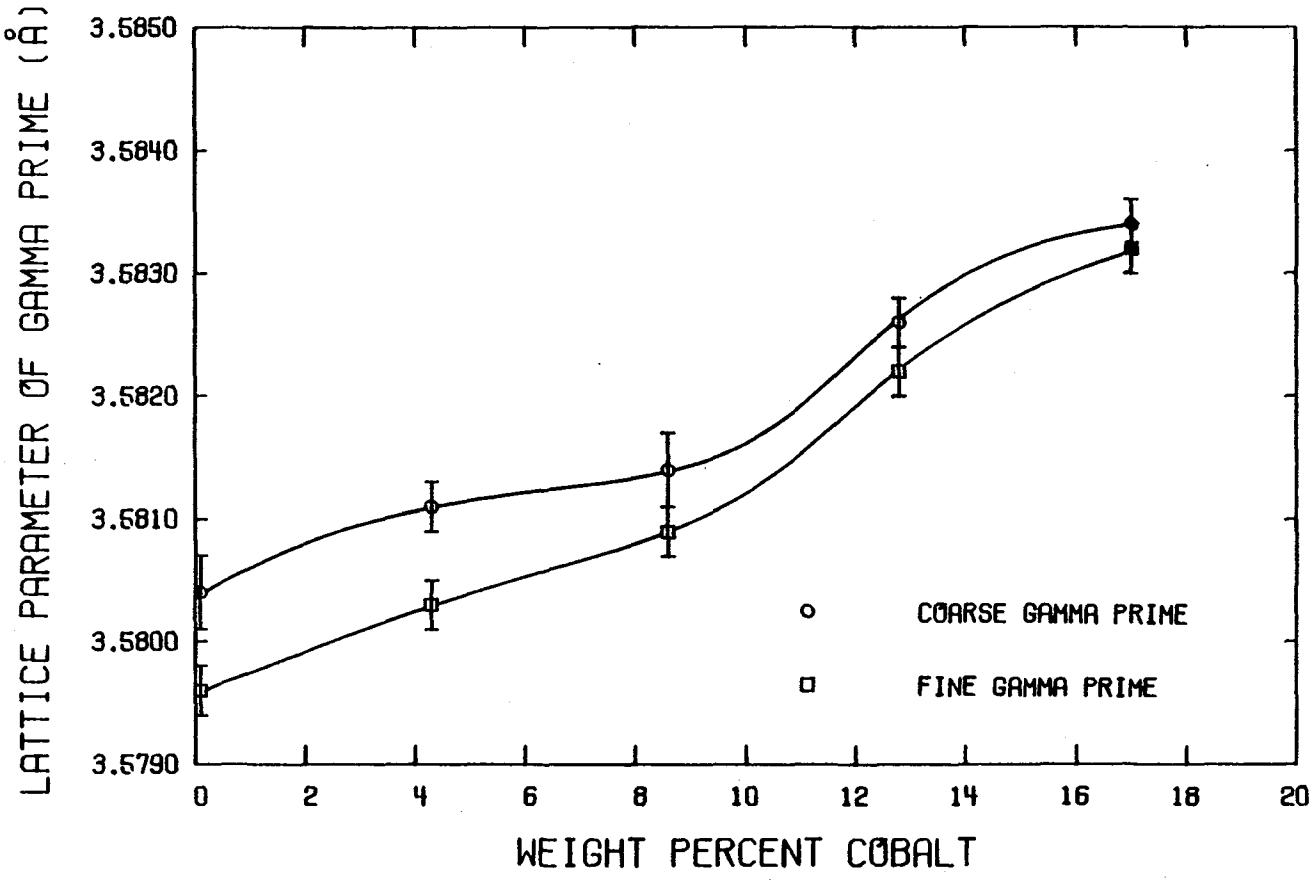

FIGURE 15. LATTICE PARAMETERS OF GAMMA PRIME IN U-700 DISK MATERIAL

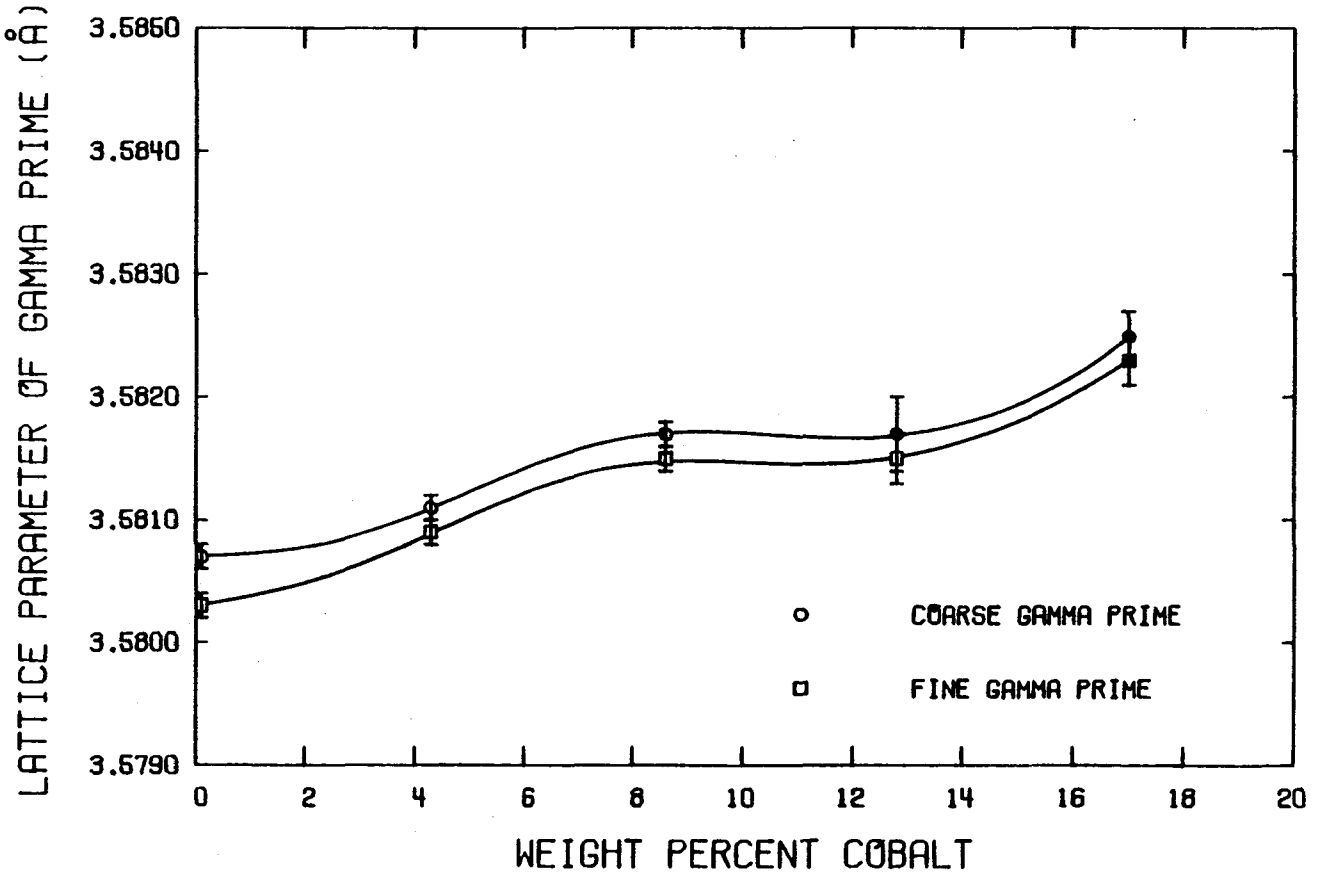

FIGURE 16. LATTICE PARAMETERS OF GAMMA PRIME IN U-700 LTA MATERIAL

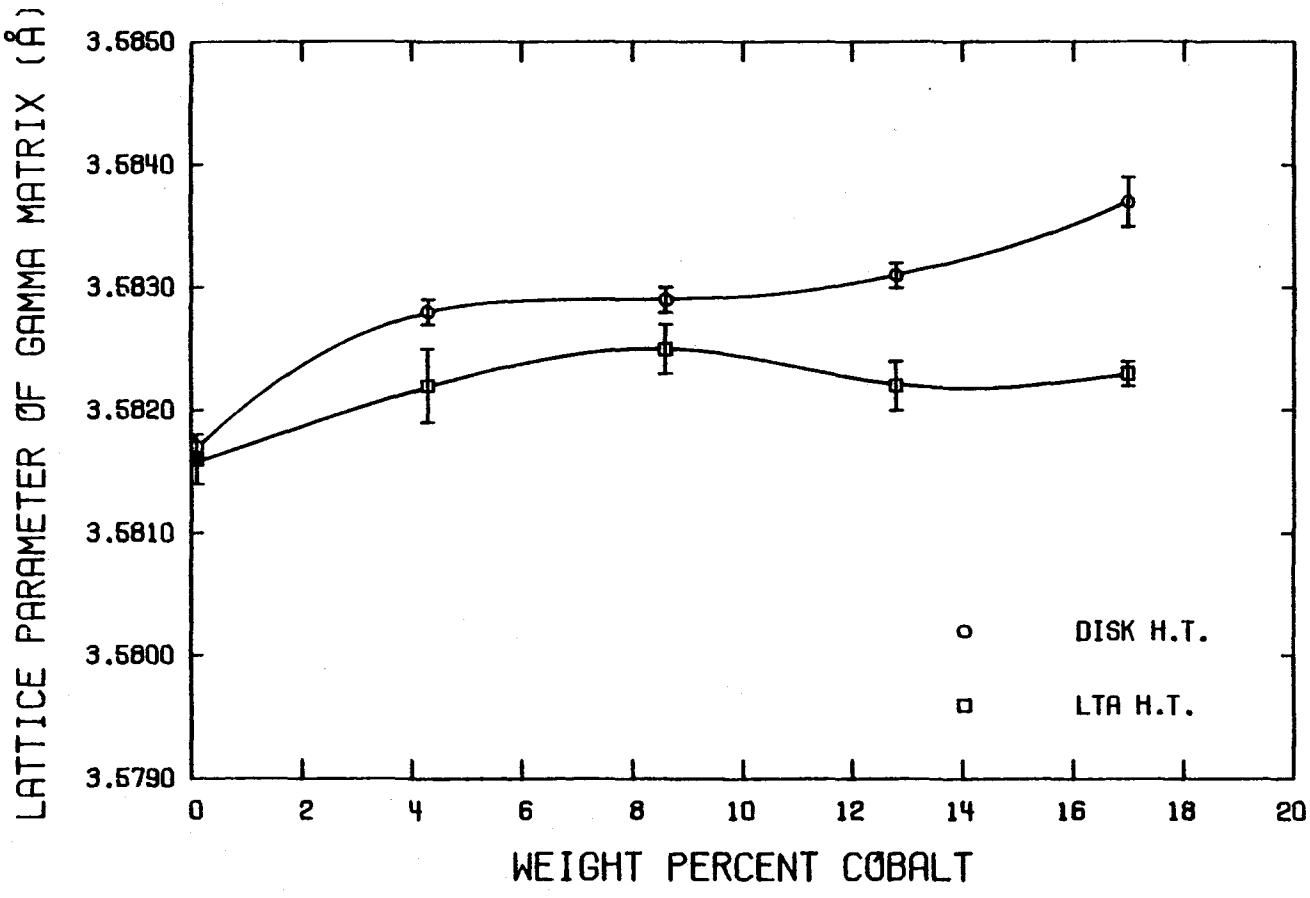

FIGURE 17. LATTICE PARAMETERS OF GAMMA MATRIX IN U-700 DISK AND LTA MATERIAL

TABLE IV. Lattice Parameters of Gamma Prime and Gamma Matrix

Wt.%Co	Disk Heat Treatment Coarse Gamma Prime (γ') a(Å) ± ESD		Fine Gamma Prime (γ') a(Å) ± ESD	
0.1	3.5804	0.0003	3.5796	0.0002
4.3	3.5811	0.0002	3.5803	0.0002
8.6	3.5814	0.0003	3.5809	0.0002
12.8	3.5826	0.0002	3.5822	0.0002
17.0	3.5834	0.0002	3.5832	0.0002
Wt.%Co	**LTA Heat Treatment Coarse Gamma Prime (γ') a(Å) ± ESD**		**Fine Gamma Prime (γ') a(Å) ± ESD**	
0.1	3.5807	0.0001	3.5803	0.0001
4.3	3.5811	0.0001	3.5809	0.0001
8.6	3.5817	0.0001	3.5815	0.0001
12.8	3.5817	0.0003	3.5815	0.0002
17.0	3.5825	0.0002	3.5823	0.0002
Wt.%Co	**Gamma Matrix Disk Heat Treatment a(Å) ± ESD**		**LTA Heat Treatment a(Å) ± ESD**	
0.1	3.5817	0.0001	3.5816	0.0002
4.3	3.5828	0.0001	3.5822	0.0003
8.6	3.5829	0.0001	3.5825	0.0002
12.8	3.5831	0.0001	3.5822	0.0002
17.0	3.5837	0.0002	3.5823	0.0001

ESD = Estimated Standard Deviation

Figures 18 and 19 graphically present the effect of cobalt on the γ/γ' mismatch in the disk and LTA heat treated alloys, respectively. This data is also listed in Table V. In general, a maximum γ/γ' mismatch was noted at 4.3 wt.% Co and, thereafter, the percent mismatch was observed to decrease with increasing cobalt content. The mismatch between the γ and fine γ' was found to be larger than the corresponding mismatch of the γ and coarse γ' in each alloy.

4.4.4. Additional Lattice Parameter Observations

The lattice parameters of the MC, $M_{23}C_6$ and M_3B_2 phases exhibit the following trends:

1. The MC carbide lattice parameter increases with increasing cobalt content.
2. The $M_{23}C_6$ carbide lattice parameter decreases with increasing cobalt content.
3. The M_3B_2 boride lattice parameter decreases with increasing cobalt content.

Table VI shows the variations of the lattice parameters of these phases found in the 0.1 and 17.0 wt.% cobalt samples.

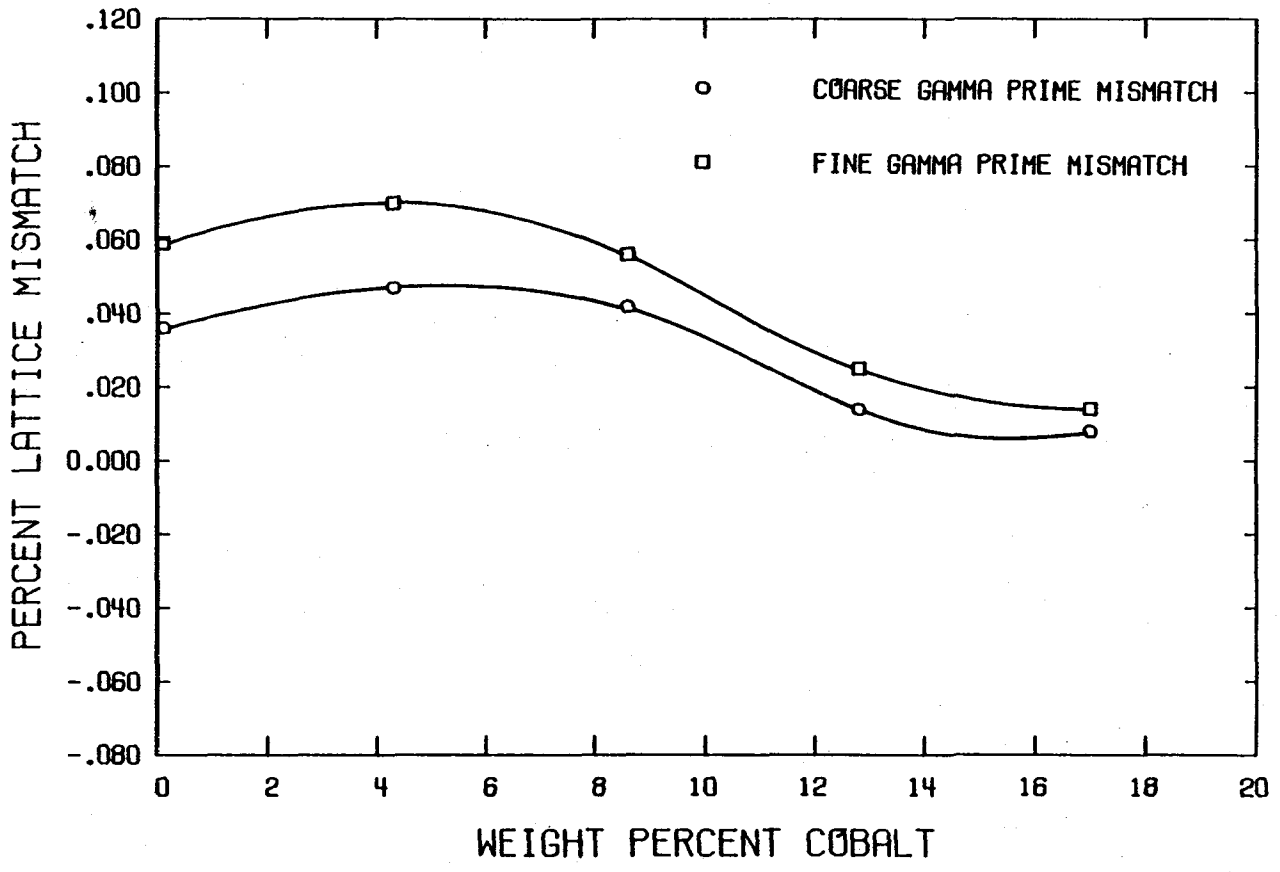

FIGURE 18. PERCENT LATTICE MISMATCH OF GAMMA/GAMMA PRIME IN U-700 DISK MATERIAL

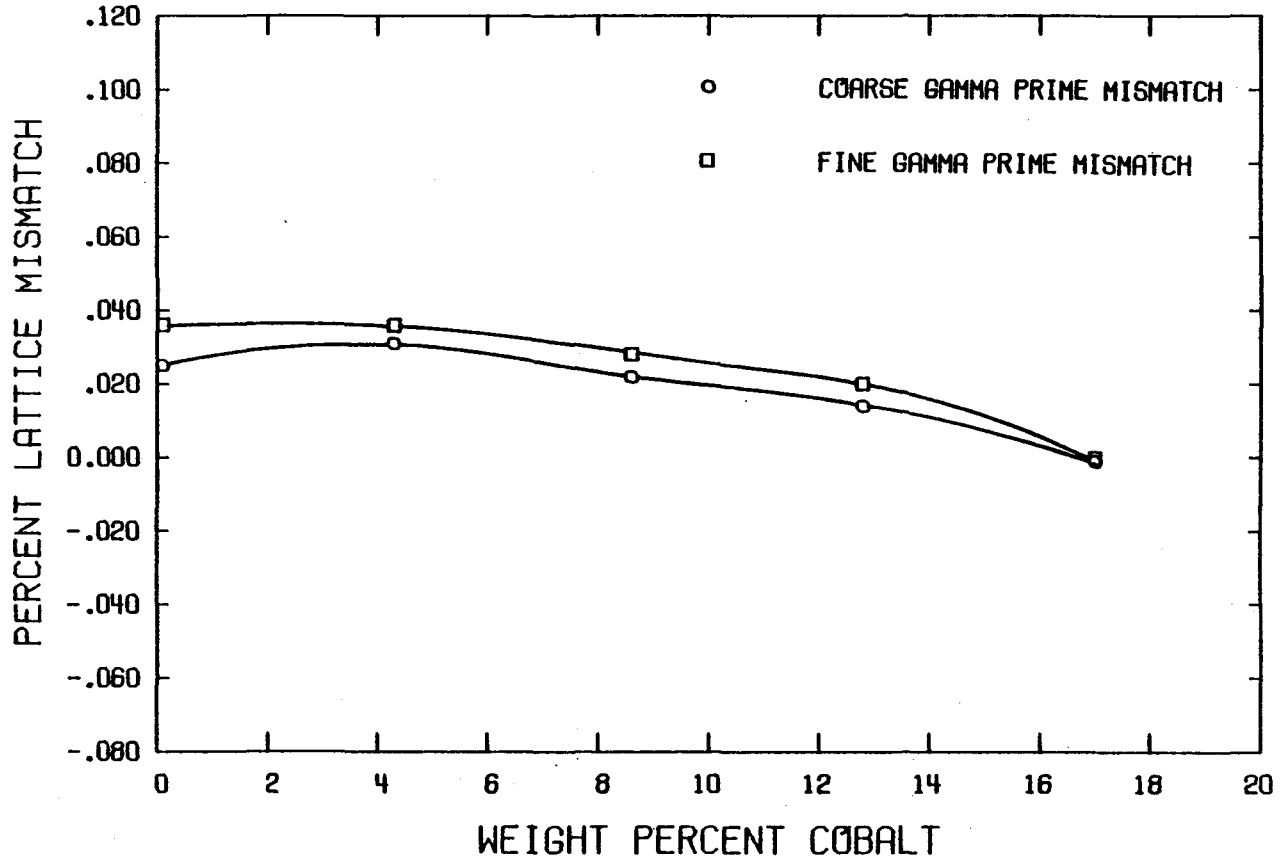

FIGURE 19. PERCENT LATTICE MISMATCH OF GAMMA/GAMMA PRIME IN U-700 LTA MATERIAL

TABLE V. Percent Lattice Mismatch of Gamma Matrix and Gamma Prime

Wt.%Co	Disk Heat Treatment Coarse Gamma Prime Mismatch (%)	Fine Gamma Prime Mismatch (%)
0.1	0.036	0.059
4.3	0.047	0.070
8.6	0.042	0.056
12.8	0.014	0.025
17.0	0.008	0.014
Wt.%Co	LTA Heat Treatment Coarse Gamma Prime Mismatch (%)	Fine Gamma Prime Mismatch (%)
0.1	0.025	0.036
4.3	0.031	0.036
8.6	0.022	0.028
12.8	0.014	0.020
17.0	- 0.001	0.000

TABLE VI. Lattice Parameters of Minor Phases

Phase	Lattice Parameter (Å)	
	0.1 wt.% Co	17.0 wt.%Co
MC	a_o = 4.30	a_o = 4.31
$M_{23}C_6$	a_o = 10.74	a_o = 10.71
M_3B_2	a_o = 5.76	a_o = 5.74
	c_o = 3.12	c_o = 3.12

V. DISCUSSION OF RESULTS

Although Udimet 700 is used for both gas turbine blade and disk applications, it is important to reiterate that this study applies only to the disk type material. Turbine disks operate at lower to intermediate service temperatures that usually are not in excess of 760°C (1400°F). At these temperatures a fine-grain size, as maintained in the disk heat treatment, enhances the mechanical properties of the material by increasing both strength and toughness.

5.1. Influence of Cobalt on the Gamma Prime (γ')

Because the γ' phase is the primary strengthener in nickel-base superalloys, it is important to understand how cobalt affects the quantity, distribution and type of γ' present in these alloys. Quantitative phase extractions of the experimental alloys of Udimet 700 show that the total weight fraction of γ' is relatively unaffected by cobalt content, especially in the disk heat treated condition. These alloys contain approximately 46 wt.% γ' after the disk heat treatment. During the long-time aging (LTA) heat treatment additional secondary γ' is precipitated, increasing the total wt.% of γ' to 47% in the lower cobalt alloys (0,4.3, and 8.6 wt.% Co). However, in the aged alloys containing 12.8 and 17.0 wt.% Co, the amount of γ' decreases to 46 and 44 wt.% γ', respectively. The reduction in the amount of γ' in the higher cobalt alloys is a result of the sigma phase which formed during the aging cycle. Sigma phase formation depletes chromium from the

γ matrix and as a result increases the solubility of aluminum and titanium in the γ matrix.

These results differ with previous studies by Heslop,[22] Maurer, et al.,[24] Nathal and Maier[25] which indicated that increasing cobalt content results in the precipitation of additional γ' in Niminoc 90, Waspaloy and Mar M-247, respectively. They concluded that cobalt decreases the solubility of the γ matrix for aluminum and titanium, the principal γ' formers, thereby increasing the precipitation of γ'. However, a recent study by Jarrett and Tien[35] shows the opposite effect for the Udimet 700 alloy. Using the same experimental alloys of Udimet 700 as used in this study, they determined that cobalt increases the solubilities for aluminum and titanium in both the matrix and γ' phases. As a result, little change was noted in the total weight fraction of γ' in these experimental alloys.

Although the overall quantity of γ' in the experimental alloys changes very little, the weight fractions and morphologies of the primary and secondary γ' phases are significantly affected by cobalt content. As cobalt is reduced, the size and quantity of the unsolutioned primary γ' increases and the amount of secondary γ' accordingly decreases. Previous studies have also indicated that cobalt reduces the coarsening kinetics of γ'.[25,28] The removal of cobalt effectively increases the solvus temperatures, resulting in earlier precipitation and longer cooling periods, which in turn allows for additional particle growth.[1]

5.2. Influence of Cobalt on the Lattice Parameters and Lattice Mismatch of the Gamma (γ) Matrix and the Gamma Prime (γ')

The lattice parameters of the γ matrix were found to increase with increasing cobalt content in the experimental alloys of Udimet 700. Cobalt has been shown to displace chromium from the γ' to the γ matrix,[28] thereby increasing the lattice parameter of the γ matrix.[34] Following the long-time aging (LTA) heat treatment, the lattice parameters of the γ matrix were reduced, as indicated in another study.[36]

Cobalt additions are also found to increase the lattice parameters of both the primary (coarse) and secondary (fine) γ' precipitates. The lattice parameters of γ' is apparently very sensitive to composition.[34,36] The lattice parameter of the primary γ' is consistently larger than those of the secondary γ' in all of the experimental alloys of Udimet 700.

The mismatch between the lattices of the γ matrix and γ' precipitates is significantly affected by the cobalt content in these experimental alloys. As the cobalt content increases, the γ/γ' mismatch decreases. Previous investigations have indicated that the γ/γ' lattice mismatch and the resultant coherency strains have an important influence on the stress rupture properties of Ni-Cr-Al alloys at elevated temperatures.[34,36] They have shown that the rupture life of these alloys can be maximized by lowering the percent mismatch to a value close to zero. This is consistent with the rupture properties of the experimental alloys of Udimet 700 reported by Jarrett and Tien,[35] where the rupture lives increased as the mismatch values decreased with increasing cobalt content.

5.3. Influence of Cobalt on the Minor Phases

Quantitative extractions of the carbides show that as cobalt is reduced in the experimental alloys of Udimet 700, the total weight percent of carbides increases only slightly. As cobalt is reduced, the solubility of the carbon in the γ matrix is decreased.[22] Hence, the lower cobalt alloys form additional carbides due to an increased amount of available carbon which is rejected from the matrix.

Cobalt, however, most significantly affects the weight fraction of the different types of carbide phases present in the experimental alloys of Udimet 700. As cobalt is reduced, the dominant carbide phase shifts from the titanium rich MC carbide to the fine grain boundary chromium rich $M_{23}C_6$ carbide and finally to the massive $M_{23}C_6$ carbide. A very abrupt transition from the fine grain boundary $M_{23}C_6$ to the massive $M_{23}C_6$ is observed as cobalt is reduced to 8.6 wt.%. It appears that this carbide transition is very close to a total transition, as very few grain boundary $M_{23}C_6$ carbides are found in the 0 and 4.3 wt.% cobalt alloys.

Other studies have revealed various effects of cobalt upon the formation of carbides which apparently may be alloy dependent. In the Nimonic alloys, a decreasing cobalt content increased the amount of the $M_{23}C_6$ carbides.[22] The opposite effect was noted in Waspaloy, where removal of cobalt decreased the amount of the $M_{23}C_6$ carbides while increasing the quantities of the MC carbides.[24] Mar M-247 exhibited an increase in the amount of carbide precipitation as the cobalt content was reduced.[25]

Cobalt also affects the phase stability of the experimental alloys of Udimet 700. During the long-time aging (LTA) heat treatment, the

sigma phase began to form in the 8.6 wt.% cobalt alloy and becomes more abundant with increasing cobalt content. In a previous study, Lund, et al.[28] similarly found that the presence of cobalt, below a critical level, inhibited sigma formation as it entered the γ' phase. And above this critical level, cobalt becomes increasingly active in the formation of the sigma phase. Lund, et al., however, found the sigma phase in a cobalt-free version of Mar M-421 contrary to that of the Udimet 700.

The M_3B_2 boride phase appears to be least affected by cobalt content in the experimental alloys. Only a slight increase in the amount of the M_3B_2 borides was found in the higher cobalt alloys.

VI. CONCLUSIONS

Nickel was substituted for cobalt in experimental alloys of Udimet 700 containing 0, 4.3, 8.6, 12.8, and 17.0 wt.% Co. Following the fine-grain disk heat treatment these alloys contained various amounts of the γ, γ', MC, $M_{23}C_6$ and M_3B_2 phases.

Cobalt was found to affect the microstructure of these experimental alloys in the following ways:

1. The total weight fraction of γ' is relatively unaffected by the cobalt content. However, as cobalt is reduced, the size and quantity of the primary-unsolutioned γ' increases and the amount of secondary-strengthening γ' decreases.
2. The lattice parameters of the γ' and γ matrix increase as cobalt is added. The lattice parameters of the primary γ' precipitates are slightly but consistently larger than those of the secondary γ'.
3. The γ/γ' lattice mismatch decreases with increasing cobalt content. The stress rupture properties at 760°C (1400°F) are maximized as the mismatch value is minimized.
4. As cobalt is reduced from the 17.0 wt.% Co level, the dominant carbide phase shifts from the titanium rich MC carbide to the chrome rich grain boundary $M_{23}C_6$ carbide and finally to the massive $M_{23}C_6$ carbide. These large massive $M_{23}C_6$ carbides, although chromium rich, contain

lesser amounts of chromium and more molybdenum than the grain boundary $M_{23}C_6$ carbides. The massive $M_{23}C_6$ carbides are found only in the low cobalt alloys, often occurring in stringers of discrete particles aligned in the rolling direction.

5. The amount of M_3B_2 borides increases slightly as cobalt is added.
6. Increasing amounts of cobalt are found in the γ, γ', MC, $M_{23}C_6$ and M_3B_2 phases as cobalt is added to these alloys.

Aging the experimental alloys at 815°C (1500°F) for 1000 hours produced the following effects:

1. The formation of a sigma phase is first observed in the 8.6 wt.% Co alloy and becomes much more abundant as the cobalt content is increased.
2. The total weight fraction of γ' is slightly increased as additional fine (secondary) strengthening γ' is precipitated during aging in the 0.1, 4.3 and 8.6 wt.% Co alloys.
3. Additional precipitation of the grain boundary $M_{23}C_6$ carbides is noted in all of the alloys aside from the cobalt-free version.

LIST OF REFERENCES

1. C. T. Sims, W. C. Hagel, The Superalloys, John Wiley and Sons, Inc. New York, 1972.

2. J. K. Tien, T. E. Howson, G. L. Chen, and X. S. Xie, "Cobalt Availability and Superalloys," Journal of Metals, pp. 12-20, October 1980.

3. J. K. Tien, R. M. Arons, and R. W. Clark, "Metals - An Endangered Species?" Journal of Metals, 28, pp. 26-28, 1976.

4. J. K. Tien, R. M. Arons, "High Temperature Superalloys - Conservation and The Ceramic Alternatives," Proceedings of the Conference on International Competition in the Management of Shrinking Resources, Ed. by W. R. Schneal, AICHE Symposium Series, Vol. 73, No. 170, 1977.

5. B. J. Reddy, "Critical Materials: Shortages, Problems and the Future," The 24th Annual International Gas Turbine Conference, San Diego, California, March 15, 1979.

6. A. G. Gray, "Four Metals at the Top of the Critical List," Metals Progress, 31, November 1979.

7. "Trends in Superalloy Technology," Technology Forcast '81, Metals Progress Press, pp. 44-46, January 1981.

8. J. R. Stephens, "NASA's Activities in the Conservation of Strategic Aerospace Materials," Proceedings of the 1980 Fall Meeting of the American Society for Metals, NASA Technical Memo 81617, October 1980.

9. A. G. Gray, "Substitution/Conservation Technology for Critical Materials, "Metals Progress, pp. 18-27, December 1981.

10. S. F. Sibley, Cobalt, Mineral Commodity Profiles, U. S. Bureau of Mines, U. S. Department of Interior, pp. 1-23, October 1979.

11. Mineral Commodity Summaries, 1969-1979, Cobalt Chapter, U. S. Bureau of Mines, January 1970 - January 1980.

12. S. F. Sibley, "Cobalt," Minerals Yearbook, U. S. Bureau of Mines, U. S. Department of Interior, 1977.

13. Mineral Trends and Forcasts, U. S. Bureau of Mines, Department of Interior, pp. 11-25, 1979.

14. R. F. Decker, "Strengthening Mechanisms in Nickel-Base Superalloys," Steel Strengthening Mechanism Symposium, Climax Molybdenum Co., 1969.

15. J. R. Mihalisin, D. L. Pasquine, "Phase Transformations in Nickel-Base Superalloys," International Symposium on Structural Stability in Superalloys, Seven Springs, PA, I, pp. 134, 1968.

16. O. H. Kriege, J. M. Baris, "The Chemical Partitioning of Elements in Gamma Prime Separated from Precipitation-Hardened, High Temperature Nickel-Base Alloys," Trans. of ASM, 62, pp. 195, 1969.

17. W. T. Loomis, The Influence of Molybdenum on the γ' Phase Formed in a Systematic Series of Experimental Nickel-Base Superalloys, Ph.D. Thesis, University of Michigan, 1969.

18. R.M.N. Pelloux, N. J. Grant, "Solid Solution and Second Phase Strengthening of Nickel Alloys at High and Low Temperatures," Trans. of AIME, 218, pp. 232, April 1960.

19. E. R. Parker, T. H. Hazlett, "Principles of Solution Hardening," Relation of Properties Microstructure, ASM, pp. 30, 1954.

20. B.E.P. Beeston, L. K. France, "The Stacking Fault Energy of Some Binary Nickel Alloys Fundamental to the Nimonic Series," Jour. Inst. Met., 96, pp. 105, 1968.

21. S. W. Wawro, MC Carbide Structures in MAR-M247, M.S. Dissertation, Purdue University, August 1981.

22. J. Heslop, "Wrought Nickel-Chromium Heat-Resisting Alloys Containing Cobalt," Cobalt, 24, pp. 128, Sept. 1964.

23. L. Habraken, D. Coutsouradis, "Tenative Synthesis on the Role of Cobalt in High-Strength Alloys," Cobalt, 26, pp. 13-15, March 1965.

24. G. E. Maurer, L. A. Jackman and J. A. Domingue, "Role of Cobalt in Waspaloy," Proceedings of the 4th International Symposium on Superalloys, Ed. by J. K. Tien, S. T. Wlodek, H. Morrow, III, M. Gell and G. E. Maurer, ASM, Metals Park, Ohio, pp. 43-52, Sept. 1980.

25. M. V. Nathal, R. D. Maier, "The Role of Cobalt in a Nickel-Base Superalloy," Case Western University/NASA Lewis Research Center, Grant NSG 3-30, May 1981.

26. E. P. Whelan, "Cobalt-Free Nickel-Base Wrought Superalloys," Proceedings of the 4th International Symposium on Superalloys, Ed. J. K. Tien, S. T. Wlodek, H. Morrow, III, M. Gell, and G. E. Maurer, ASM, Metals Park, Ohio, pp. 53-62, Sept. 1980.

27. F. F. Kimushin, "Heat Resisting Steels and Alloys," Metallurgia, Moscow, U.S.S.R., 1969.

28. C. H. Lund, M. J. Woulds, and J. Hoskin, "Cobalt and Sigma: Participant, Spectator, or Referee?" Proceedings of the 1st International Symposium on Structural Stability in Superalloys, Seven Springs, PA, pp. 25-46, 1968.

29. J. F. Radavich, R. R. Watkins and L. M. Keilman, Proceedings of the 5th Annual Purdue University Student-Industry High Temperature Materials Seminar, School of Materials Engineering, Purdue University W. Lafayette, IN, pp. 122-139, 1979.

30. M. J. Donachie, O. H. Kriege, "Phase Extraction and Analysis in Superalloys - Summary of Investigations by ASTM Committee E-40 Task Group I," Jour. of Materials, 7, pp. 269-279, 1972.

31. M. J. Donachie, "Phase Extraction and Analysis in Superalloys - 2nd Summary of Investigations by ASTM Subcommittee E04.91," Jour. of Testing and Evaluation, JTEUA, 6, pp. 189-195, May 1978.

32. O. H. Kriege and C. P. Sullivan, "The Separation of Gamma Prime From Udimet 700,: Trans. ASM, 61, pp. 278-282, 1968.

33. D. E. Williams, LCR-2 Lattice Constant Refinement Program, U. S. Atomic Energy Commission, Iowa State Research and Development, Report No. 1052, Now. 1964.

34. G. N. Maniar, J. E. Bridge, Jr., H. M. James, and G. B. Heydt, "Correlation of Gamma-Gamma Prime Mismatch and Strengthening in Ni/Fe-Ni Base Alloys Containing Aluminum and Titanium as Hardeners," Metallurgical Trans. of ASM, 1, pp. 31-42, January 1970.

35. R. N. Jarrett, J. K. Tien, "Effects of Cobalt on Structure, Michrochemistry and Properties of a Nickel-Base Superalloy," to be published.

36. G. N. Manier, J. E. Bridge, Jr., "Effect of Gamma-Gamma Prime Mismatch, Volume Fraction Gamma Prime, and Gamma Prime Morphology on Elevated Temperature Properties of Ni, 20 Cr, 5.5 Mo, Ti, Al Alloys, Metallurgical Trans. of ASM, 2, pp. 95-102, January 1971.

APPENDIX

1. Sample Preparation for Extractions.

   Duplicate extraction samples which had been sectioned from the experimental alloys were ground through a 120 grit silicon carbide abrasive to remove possible surface contaminants such as flow metal. The duplicate samples were simultaneously extracted, and the resultant residues were analyzed and compared for consistency.

2. Procedure for the EX-1 Extraction.

   The prepared samples, as described in the previous section, were suspended via resistance welded platinum wires in separate 250 ml beakers containing a 10% Hydrochloric Acid-Methanol electrolyte. The extraction specimens remained submerged in the electrolyte throughout the entire two hour extraction period. Tantalum sheet was used as the cathode material. In order to prevent matrix contamination, the standard current density of 0.07 Amps/cm^2 had to be altered according to the cobalt content of the experimental alloys as indicated in Section 3.3.1. The optimum current density for each alloy was continuously monitored and maintained throughout the extraction period. At thirty minute extraction intervals, the residues adhering to the specimens were removed by ultrasonic agitation in separate beakers containing methonal. After a total of two hours of extraction, the resultant residues in the electrolyte and from ultrasonic agitation were filtered through solvent

resistant 0.6 μm Millipore filters and thoroughly rinsed.

The overall weight loss and weight of extracted residue from each specimen was noted. The method used to determine the weight percent of extracted residue for each extraction was as follows:

$$\text{wt.\% Ext. Res.} = \frac{\text{Residue wt. + wt. loss of Filter Pad}}{\text{Wt. loss of Extracted Sample}} \times 100\% \quad (1)$$

3. Procedure for the EX-2 Extraction.

After following the extraction sample preparation as described in Section 1 of the Appendix, each specimen was immersed in 100 ml of a 10% Bromine-Methonal reagent and allowed to react for thirty minutes. [Caution -- it is extremely important that this extraction be done within a well ventilated hood.] The solution and residue were then carefully transferred to a separate beaker while the specimen remained in its original extraction beaker. The remaining specimen and extraction beaker were thoroughly rinsed with methanol. The solution containing the extracted residue was then filtered along with the residue which had been rinsed from each sample. The residues were filtered through 0.6 μm pore size solvent resistant membrane filters and were again thoroughly rinsed with methonal. The final weights of the specimens and extracted residues were used to determine the weight percent of extracted residue from each extraction using Eq. (1), as described previously.

4. Procedure for the Gamma Prime (γ') Extraction.

The extraction samples were prepared as described in Section 1 of the Appendix, and suspended via resistance welded platinum wires in 250 ml beakers containing an electrolyte which consisted of 1% Ammonium Sulfate (by weight) and 1% Citric Acid in deionized water.

A tantalum sheet was used as the cathode material. The extraction specimens remained submerged in the electrolyte throughout the three hour room temperature extraction, while a current density of 0.03 Amps/cm^2 was applied. After completing the extraction, the samples and adhering γ' residues were transferred to beakers of deionized water and soaked for twenty minutes to remove the remaining electrolyte. The small amount of γ' remaining in the electrolyte and in the soaking beakers was recovered via filtration through 0.6 μm pore size filters. Each specimen with the adhering γ' was weighed after it had been allowed to thoroughly dry. Subsequently, the dried γ' was removed from each sample with a scalpel. Then the samples were ultrasonically agitated in water and finally nylon brushed to remove any remaining γ'. The dry weights of the specimen before and after scraping were recorded and the respective weight fraction of γ' was determined by difference.

The extracted γ' residue obtained using this technique is also accompanied by a minor amount of the phases normally extracted in the EX-1 type extraction. In order to determine the weight percent of extracted γ'. The weight percent of the EX-1 type residue must be subtracted from the total weight percent of extracted residue as follows:

$$\text{Wt.\% Ext. Res.} = \frac{\text{Residue Weight}}{\text{Weight Loss of Sample}} \times 100\% \qquad (2)$$

$$\text{Residue Wt.} = \text{Wt.}_f(\text{Extd. Sample} + \gamma') - \text{Wt.}_f(\text{Extd. Sample} - \gamma') + \text{Wt.}_f(\gamma' \text{ Collected on Filter Pad}) \qquad (3)$$

$$\text{Wt.Loss of Sample} = \text{Wt.}_i\text{(Sample)} - \text{Wt.}_f\text{(Extd. Sample - } \gamma') \quad (4)$$

$$\text{Corrected Wt.\%}\gamma' = \text{Wt.\% Ext. Res. - Wt.\% EX-1 Res.} \quad (5)$$

5. Separation of the Coarse and Fine Gamma Prime (γ') Particles.

The lattice parameters of the primary (coarse) and secondary (fine) γ' phases in the experimental alloys were determined using samples of the extracted γ' which had been separated by particle size. The extracted γ' residues from each of the alloys were initially placed in methanol and ultrasonically agitated for one minute to break up any agglomerated particles. After the particles were allowed to settle for five minutes, a portion of the fine γ' particles left in suspension was drawn from the top of the solution and retained for subsequent XRD sample preparation. Additional methonal was added to the solution which was again ultrasonically agitated, allowed to settle for five minutes and the residue left in suspension was again drawn off. This procedure was repeated until all of the fine γ' had been removed and only the coarse γ' remained at the bottom of the beaker. The solutions containing the isolated coarse and fine γ' particles were then filtered through 0.6 μm pore size filter paper and prepared for XRD analysis.

1. Report No.	2. Government Accession No.	3. Recipient's Catalog No.
NASA CR-165605		

4. Title and Subtitle	5. Report Date
EFFECTS OF COBALT ON THE MICROSTRUCTURE OF UDIMET 700	June 1982
	6. Performing Organization Code
7. Author(s)	8. Performing Organization Report No.
Mayer Abraham Engel	None
	10. Work Unit No.
9. Performing Organization Name and Address	
Purdue University Department of Material Engineering West Lafayette, Indiana	11. Contract or Grant No.
	NAG3-57
	13. Type of Report and Period Covered
12. Sponsoring Agency Name and Address	Contractor Report
National Aeronautics and Space Administration Washington, D. C. 20546	14. Sponsoring Agency Code
	510-57-12B

15. Supplementary Notes

Final report. Project Manager, Coulson M. Scheuermann, Materials Division, NASA Lewis Research Center, Cleveland, Ohio 44135. Based on a thesis submitted as partial fulfillment of the requirements for the degree of Master of Science to Purdue University, West Lafayette, Indiana in 1981.

16. Abstract

The objective of this study was to determine the effects of cobalt on the microstructure of Udimet 700, a high temperature nickel-base superalloy. Cobalt, a critical and "strategic" alloying element in many superalloys, was systematically substituted by nickel in experimental alloys of Udimet 700 containing 0.1, 4.3, 8.6, 12.8 and the standard 17.0 wt.% cobalt. Electrolytic and chemical extraction techniques, X-ray diffraction, scanning electron and optical microscopy were used for the microstructural studies. The total weight fraction of gamma prime(γ') was not significantly affected by the cobalt content, although a difference in the size and quantities of the primary and secondary γ' phases was apparent. The lattice parameters of the γ' were found to increase with increasing cobalt content while the lattice mismatch between the gamma (γ) matrix and γ' phases decreased. Other significant effects of cobalt on the weight fraction, distribution and formation of the carbide and boride phases as well as the relative stability of the experimental alloys during long-time aging are also discussed.

17. Key Words (Suggested by Author(s))	18. Distribution Statement
Nickel-base alloys; Cobalt effects; Phase characterization; Gamma; Gamma prime; Carbides; Microstructure	Unclassified - unlimited STAR Category 26

19. Security Classif. (of this report)	20. Security Classif. (of this page)	21. No. of Pages	22. Price*
Unclassified	Unclassified	66	

* For sale by the National Technical Information Service, Springfield, Virginia 22161